NASA TECHNICAL NOTE

NASA TN D-7601

NASA TN D-7601

ASSESSMENT OF AN ANALYTICAL PROCEDURE FOR PREDICTING SUPERSONIC EJECTOR NOZZLE PERFORMANCE

by Bernhard H. Anderson

Lewis Research Center
Cleveland, Ohio 44135

NATIONAL AERONAUTICS AND SPACE ADMINISTRATION • WASHINGTON, D. C. • APRIL 1974

1. Report No.	2. Government Accession No.	3. Recipient's Catalog No.
NASA TN D-7601		

4. Title and Subtitle	5. Report Date
ASSESSMENT OF AN ANALYTICAL PROCEDURE FOR PREDICTING SUPERSONIC EJECTOR NOZZLE PERFORMANCE	APRIL 1974
	6. Performing Organization Code

7. Author(s)	8. Performing Organization Report No.
Bernhard H. Anderson	E-7413
	10. Work Unit No. 501-24

9. Performing Organization Name and Address	11. Contract or Grant No.
Lewis Research Center National Aeronautics and Space Administration Cleveland, Ohio 44135	
	13. Type of Report and Period Covered: Technical Note

12. Sponsoring Agency Name and Address	14. Sponsoring Agency Code
National Aeronautics and Space Administration Washington, D.C. 20546	

15. Supplementary Notes

16. Abstract

An investigation has been carried out to assess the ability of analysis to predict ejector nozzle characteristics over a wide range of conditions and to study the relation between design parameters and performance. In general, the analytical method investigated provided an accurate and economical method for predicting the performance of supersonic ejector nozzles. It was also concluded that the factors which had the greatest influence over ejector nozzle behavior were those which influenced the initial expansion and recompression process.

17. Key Words (Suggested by Author(s))	18. Distribution Statement
Aerodynamics Propulsion Supersonic Ejector nozzles	Unclassified - unlimited CAT.28

19. Security Classif. (of this report)	20. Security Classif. (of this page)	21. No. of Pages	22. Price*
Unclassified	Unclassified	50	$3.25

* For sale by the National Technical Information Service, Springfield, Virginia 22151

ASSESSMENT OF AN ANALYTICAL PROCEDURE FOR PREDICTING SUPERSONIC EJECTOR NOZZLE PERFORMANCE

by Bernhard H. Anderson

Lewis Research Center

SUMMARY

An investigation has been carried out to assess the ability to compute ejector nozzle performance over a wide range of geometries and flow conditions of interest. In addition, a study was performed which dealt with the interrelation between various ejector nozzle design parameters and performance. In making the evaluation, comparisons between theory and experiment were made so that the importance of both the various analytical assumptions and the design variables becomes apparent.

In general, the analytical method investigated can provide an accurate and economical means for designing supersonic ejector nozzles over a wide range of conditions of interest. Two factors that have been shown to strongly influence nozzle performance are the primary nozzle inlet flow field and the mixing process between the primary and secondary flow fields. In general, the initial expansion and recompression process dominates ejector performance. Therefore, any factors such as primary nozzle lip angle, spacing ratio, shroud shoulder diameter ratio, and so forth, which affect these processes strongly influence ejector performance.

INTRODUCTION

A continuing problem in the development of exhaust nozzle systems is the large number of design parameters that the engineer must consider in order to optimize an ejector nozzle. Not only is the design engineer faced with building an effective ejector nozzle, but frequently he must modify the design to satisfy requirements over which he has little control and which often compromise nozzle performance. Often lacking practical analytical solutions, the engineer will rely almost exclusively on experimental data acquired at great cost. These data usually serve as a useful design tool within the class of flow conditions and geometries tested. However, considering the large num-

ber of independent variables which can affect nozzle performance, such as area ratio, length ratio, shroud geometry, shroud shoulder diameter ratio, spacing ratio, primary nozzle geometry, weight flow ratio, temperature ratio, Reynolds number, and so forth, it is self-evident that sufficient experimental data to cover the vast number of design possibilities will not be forthcoming. Clearly, the development of better analytical tools will benefit the design engineer by allowing him to conduct parametric studies so that the interrelation between the design parameters and performance may be examined at greatly reduced development time and cost.

With the exception of reference 1, little attempt has been made to make a systematic assessment of ejector flow theory and how well it applies within the range of ejector geometries and flow conditions of interest. There have been numerous analytical methods proposed for describing the ejector nozzle flow field (refs. 2 to 6), and some of the difficulties encountered in these procedures are discussed in reference 7. However, the most recent and more usable analyses (refs. 3, 5, and 6) use the phenomenological description of the flow field and mixing processes presented in reference 5. This description was later extended in reference 7 to be somewhat more general so that it would be of greater value in ejector studies. It is apparent from the results of reference 1 that the basic approach used in reference 7 is capable of predicting ejector nozzle performance with sufficient accuracy for engineering use for the number of ejectors considered. Although a considerable amount of experimental data exist on the pumping and exhaust characteristics for various ejector configurations, much of these data are contradictory or unusable because of insufficient documentation. However, the data presented in references 8 to 10 were found to form a reliable set of measurements.

Therefore, this investigation was conducted to further assess the ability of the analysis presented in reference 7 to predict nozzle performance over a wider range of ejector geometries and flow conditions and to continue studying the relation between the various ejector design parameters and nozzle performance. In making the evaluation, comparisons between theory and experiment are made so that the importance of both the various analytical assumptions and the design variables becomes apparent.

SYMBOLS

A area

A_p primary nozzle exit area

A_S shroud shoulder area

C_v nozzle efficiency, $(F - p_0 A_e)/(F_{ip} + F_{is})$

D diameter

D_p primary nozzle exit diameter

D_S shroud or shoulder diameter

F thrust

F_{ip} ideal thrust based on measured primary flow

F_{is} ideal thrust based on measured secondary flow

L_S distance from primary nozzle exit to shroud shoulder point

M Mach number

P total pressure

p static pressure

R radius

Re Reynolds number based on primary nozzle exit diameter

T total temperature

W weight flow

W_p primary weight flow

W_{ip} ideal primary weight flow

X axial distance

Y radial distance

α_p primary nozzle lip angle

δ^* displacement thickness

$\omega\sqrt{\tau}$ corrected secondary weight flow ratio, $\frac{W_s}{W_p}\sqrt{\frac{T_s}{T_p}}$

Subscripts:

e exit

i ideal

p primary

S shroud or shoulder

s secondary

0 free-stream or reference conditions

Superscript:

* sonic conditions

RESULTS AND DISCUSSION

Ejector Nozzle System

The flow within an ejector nozzle is based on the mutual interaction between a high-energy primary flow and a low-energy secondary flow, figure 1. The two streams begin to interact at the primary nozzle lip. For the ejector operating in the supersonic regime, the secondary flow is effectively "sealed off" from ambient conditions, and the ejector mass flow characteristics depend only on the ratio of secondary to primary total pressure. The form of this dependence is called the pumping characteristics, and they define an ejector operating limit line. Thus, for a given ejector nozzle configuration, the pumping characteristics define the maximum amount of flow that can be "pushed" through the secondary passage at a given secondary total pressure. When the ejector nozzle operates at a mass flow ratio less than the maximum value defined by the pumping curve, the primary flow detaches from the shroud wall. Thus, the ejector flow field depends on ambient conditions. The pumping characteristics, and consequently the thrust characteristics, can be influenced by a great many geometric as well as aerodynamic variables. The influence of these variables on nozzle performance, in addition to factors which will affect the analysis of ejector systems, is discussed in the following sections.

Influence of Sonic Line and Mixing

The influence of both the sonic-line assumptions and the mixing process on the performance of a convergent-divergent contoured flap ejector nozzle is shown in figure 2. The ejector nozzle had a shoulder diameter ratio D_S/D_p of 1.37, and the shroud was located at a spacing ratio L_S/D_p of 0.5. Shroud coordinate points for this ejector configuration are presented in table I. The term "mixing" in figure 2 indicates that the mixing between the two streams was computed as an interaction analysis (ref. 7), while the "no mixing" solution is indicative of an inviscid computation. The "real" sonic-line solution was based on choked flow through a conical primary nozzle with an angle of 27°, while the "plane" sonic-line solution assumed uniform flow discharging axially from the primary nozzle. For ejector nozzles whose shroud or shoulder diameter D_S is large compared to the primary nozzle diameter D_p, the effect of mixing can be very important to both the pumping and thrust characteristics, as indicated in figure 2. For both the real and plane sonic-line solutions, higher thrust and nozzle efficiency were computed for the no-mixing cases primarily because of the higher secondary pressures, as indicated by the pumping characteristics in comparing the real and plane sonic-line solutions. It is readily apparent that the sonic-line assumptions can substantially affect the calculation of the pumping and stream thrust characteristics. The much larger

stream thrust that was computed for the plane sonic-line cases was caused by the higher primary nozzle mass flow. Because the actual mass flow was used in evaluating thrust efficiency, these sonic-line differences were not as apparent in the thrust efficiency characteristics. The differences that did occur, however, were probably caused by both divergence losses in the primary inlet flow and mismatching of the ejector flow field with the shroud wall. Thus, both the mixing process and the primary inlet flow strongly affect the pumping characteristics, while the mixing process has a greater effect on nozzle efficiency than the sonic line. In general, the real sonic-line mixing solution compared favorably with ejector nozzle data from reference 8.

The measured and computed static pressure distributions on the shroud surface are compared in figure 3 for the same four cases. As would be expected, the differences that occurred in the pumping characteristics also show in the static pressure distribution. For secondary weight flow ratios of 0 and 0.02, the analysis (solid line) was able to predict reasonably well both the location and magnitude of the shock, or recompression pressure rise, associated with primary flow impingement over the secondary shroud. Although the analysis predicted the secondary inlet flow conditions quite well at a secondary weight flow ratio of 0.04, it was unable to locate the recompression region. However, the agreement with both the pumping and thrust characteristics is quite good at this secondary weight flow ratio. At the high secondary weight flow ratio of 0.10, where the mechanism for isolating the secondary flow from ambient conditions is aerodynamic choking, agreement between the measured and calculated (solid line) static pressure distributions is very good.

The influence of secondary weight flow ratio on the flow field of the same convergent-divergent contoured flap ejector nozzle is shown in figure 4. Each line segment in these computer flow-field plots represents a Mach number vector whose length is proportional to the local Mach number and whose angle is the local flow angle. The recompression shock that formed just off the shroud shoulder is clearly visible at a secondary weight flow ratio of 0. As the secondary weight flow ratio increases, the recompression shock pulls away from the shroud wall and forms further downstream until it is no longer visible within the flow field that was plotted.

The influence of both the sonic-line assumption and the mixing process is presented in figure 5 for a convergent-divergent conical flap ejector having a shoulder diameter ratio D_s/D_p of 1.225 and operating at a Reynolds number Re of 4.0×10^6. The real sonic-line solutions were based on choked flow through a conical primary nozzle with a lip angle of 16°. Qualitatively, the effects of the primary inlet flow condition and the mixing process resulted in trends similar to those of the previous ejector nozzle example although the pumping characteristics were influenced more by the sonic-line assumptions than by mixing at the higher secondary flow rates. However, at the lower secondary flow rates, where it may be advantageous to operate this ejector, the effects of mixing on nozzle performance can be very important and thus can not be ignored or assumed

to be neglibible.

Figure 6 shows the influence of secondary weight flow ratio on the flow field of this conical flap ejector nozzle. The same qualitative flow behavior was found to exist in this conical flap ejector as in the previous contoured flap ejector nozzle.

The sonic line depends not only on the primary nozzle geometry, but also on the back pressure under which the nozzle is operating. For ejector nozzles this back pressure is a function of secondary weight flow ratio. This dependence is illustrated in figure 7, where the primary nozzle flow coefficient is shown as a function of ejector corrected secondary weight flow ratio for both theory and data. The experimental data (fig. 7(b)) were obtained for a primary nozzle with a 27° inside lip angle operating within an ejector at a Reynolds number of 3.3×10^{6}. The theoretical calculations were obtained by integrating the mass flux along the computed sonic line and correcting for boundary layer effects according to the analysis of reference 7. The boundary layer, or Reynolds number, effect is represented by the difference between the dashed line and a discharge coefficient of 1.00. The calculations indicate about a 0.4 percent decrease in discharge coefficient when the corrected secondary weight flow ratio was increased from 0 to 10 percent. This decrease was caused by an increase in the back pressure under which the primary nozzle was operating. The measured data from reference 8 indicate this variation. The conical flap ejector nozzle of reference 9 (fig. 7(a)) had a primary nozzle with a lip angle of 16°, and therefore the discharge coefficient was not as sensitive to secondary flow rate as the previous ejector nozzle configuration.

The differences between the real and plane sonic-line solutions become readily apparent by comparing the computer flow-field plots for the real and plane sonic-line cases, figure 8. At the same corrected secondary weight flow ratio, the recompression shock that forms after the initial primary flow expansion will always be located further downstream for the real sonic solution, where the shock losses will be greater. The assumption that the primary inlet flow follows a Prandtl-Meyer expansion around the nozzle lip from a uniform state is very limiting because it can not represent the character of the ejector flow field formed from flow discharging from a choked conical nozzle. Because the real sonic-line solution will always give a smaller primary mass flow rate, the ejector nozzle will always appear overexpanded when compared to the plane sonic-line solution at the same ejector mass flow ratio. This overexpansion effect can be seen in figure 9, which presents the exit Mach number profiles for both the conical flap ejector nozzle (fig. 9(a)) and the contoured flap ejector nozzle (fig. 9(b)).

A somewhat similar interpretation can also be applied to the effects of mixing within supersonic ejector nozzles. Although the mixing process can not change the total ejector mass flow rate, as is the case with the sonic-line assumption, the primary flow exit Mach number profiles for the mixing solutions always appear overexpanded when compared to the no-mixing solution. Thus, the mixing process makes the ejector nozzle appear to be operating at a lower secondary weight flow ratio. This interpre-

tation of the mixing process led to the phenomenological description presented in reference 5.

The conceptual idea that an ejector flow with mixing is equivalent to an inviscid flow at a lower secondary weight flow ratio can also be applied to the sonic-line problem. By resizing the primary nozzle so that both the primary nozzle mass flow rate and the ejector mass flow ratio are matched to known values, an equivalent ejector can be defined. However, the thrust inventory must be performed over actual geometry. And thus the accounting for the difference between the actual and effective primary nozzle exit areas is left in doubt.

Influence of Primary Nozzle Lip Angle

The idea that problems associated with calculation of a sonic line can be avoided by replacing the actual ejector nozzle with an equivalent nozzle which matches the primary mass flow rate and ejector nozzle mass flow ratio but which has a plane sonic line is examined in figure 10. The ejector nozzle performance presented in figure 10 was determined for the same convergent-divergent conical flap ejector that was examined in figure 5. This ejector had a shoulder diameter ratio D_S/D_p of 1.225 and a spacing ratio L_S/D_p of 0.22. The nozzle performance for the ejector which had a choked primary nozzle (solid line) was obtained by keeping the primary nozzle exit area constant so that the shoulder diameter ratio, the spacing ratio, and the exit area ratio were constant as the lip angle was increased from 0^o to 60^o. Computer predictions for the choked conical primary nozzle, which were done at a secondary weight flow ratio of 0.04, indicated that this variation in lip angle resulted in a 27 percent increase in pumping, a 1.3 percent decrease in nozzle efficiency, and a decrease of nearly 22 percent in the primary nozzle mass flow rate. With the primary nozzle mass flow characteristics known, an equivalent plane sonic-line nozzle was defined by decreasing the primary nozzle exit area so that the same mass flow could be achieved at the secondary weight flow ratio of 0.04. This was accomplished by replacing the primary nozzle exit area A_p by the value $(W_p/W_{ip})A_p$, where W_p/W_{ip} is the primary nozzle flow coefficient, and setting the lip angle to 0^o. Thus, for this set of predictions (represented by the dashed line), the shoulder diameter ratio D_S/D_p, the ejector spacing ratio L_S/D_p, and the ejector area ratio A_e/A_p all increased. The increase in these parameters, however, did not increase the pumping action sufficiently to match the secondary total pressure ratio or thrust efficiency characteristics of the actual ejector nozzle (solid line). Since the ejector with the choked conical primary nozzle is already operating at the optimum spacing ratio L_S/D_p, no further gains are possible.

The concept of equivalent ejector nozzles is not a very good approximation to use to avoid the problem of calculating a starting sonic line. However, two definite conclusions

can be reached about the nature of supersonic ejector nozzles: (1) nozzle efficiency depends on both the primary nozzle mass flow rate and nonuniformities in the entrance flow field and (2) at the same mass flow rate a smaller uniform-flow primary nozzle will always improve ejector efficiency. To further delve into the nature of ejector nozzles, the exit Mach number profiles from the previous study are shown in figure 11, for primary nozzle lip angles ranging from 10° to 60°. As would be expected, when the primary nozzle lip angle increased, a greater portion of the exit flow appeared to be overexpanded, and hence the average exit Mach number increased. This was clearly caused by the effective ejector nozzle area ratio increasing because the primary nozzle flow coefficient was decreasing. However, the character of the distortion of the exit plane did not change appreciably.

The influence of the primary nozzle lip angle on the ejector flow field is presented in figure 12 and indicates that the sonic line can vary considerably. It is also interesting to note that, even for the 10° primary nozzle, there is noticable distortion in the sonic line.

Influence of Spacing and Shoulder Diameter Ratio

The location of the shroud shoulder relative to the primary nozzle exit (spacing ratio) L_S/D_p, together with the shoulder diameter ratio D_S/D_p, is critical in attaining high nozzle performance because it controls the initial expansion of the exhaust gas and has a strong influence on secondary airflow pressures. In order to systematically study the effects of these two design variables, a series of calculations were performed on a family of five conical flap ejector nozzles, figure 13, and compared to both published and unpublished data obtained in the tests reported in reference 9. The shoulder diameter ratio of these nozzles varied from 1.183 to 1.342, while all had a 9° half-angle conical expansion section and thus an exit area ratio A_e/A_p of 2.75. The exact shroud contours that were used in the calculation are presented in tables II to VI.

For each shroud configuration shown in figure 13, data and calculations are presented in figures 14 to 18 at secondary weight flow ratios of 0.025, 0.04, 0.06, and 0.10. At each shoulder diameter ratio D_S/D_p and secondary weight flow ratio $\omega\sqrt{\tau}$, the spacing ratio L_S/D_p was increased from 0 to 0.7. While increasing the spacing ratio did result in higher secondary pressure, and consequently higher thrust contributions, this effect was offset by a decreasing integrated pressure force along the shroud wall in the thrust direction. The net result was that the efficiency maximized at a particular spacing ratio. For the shroud contour which had a shoulder diameter ratio of 1.183 (fig. 14), the optimum spacing ratio was about 0.2. But when the shoulder diameter ratio was increased to 1.225 (fig. 15), the optimum spacing ratio increased to about 0.3.

According to the calculations, the pumping characteristics also exhibit the property that secondary total pressure will maximize with spacing ratio (figs. 14(d) and 15(d)), but the maximum total pressure occurred at a higher spacing ratio than the maximum efficiency. As the spacing ratio was increased, the divergent portion of the shroud exhibited less influence over the pumping characteristics until a point was reached when the ejector flow was controlled primarily by the convergent segment of the shroud wall. It is also apparent from figures 14 to 18 that both the secondary weight flow ratio and the shoulder diameter ratio have a strong influence over this process. This fact would seem to suggest that a good way to improve the pumping action of an ejector would be to constrict the exit. However, gains in nozzle efficiency would not be realized.

The role of the spacing ratio in controlling thrust efficiency is examined in figure 19 by presenting the exit Mach number profiles at selected shroud positions relative to the primary nozzle exit plane. The calculations were performed for the ejector having the shroud configuration with a shoulder diameter ratio of 1.225 and operating at a secondary weight flow ratio of 0.04. The exit Mach number corresponding to the geometric area ratio of 2.75 was about 2.54. At a spacing ratio L_S/D_p of 0, there existed an overexpanded region in the core of the primary flow field. As the spacing ratio was increased, this overexpanded region diminished in size until an almost flat Mach number profile existed. This condition occurred at a spacing ratio L_S/D_p of 0.3, which corresponded to the condition of maximum efficiency. As the spacing ratio was increased beyond this optimum point, a large underexpanded region developed in the core of the ejector flow field. This region was caused by the recompression shock forming inside the flow field enclosed by the shroud. Beyond a spacing ratio of 0.4, these shocks were sufficiently strong to cause subsonic conditions in the primary flow field. In summary, it appears that the spacing ratio L_S/D_p determines the characteristic distortion patterns at the ejector nozzle exit and that peak performance will occur when this distortion is minimized.

Computer plots showing the effect of spacing ratio on the flow field of the ejector nozzle having the shroud configuration with the shoulder diameter ratio of 1.225 are presented in figure 20. The performance for this ejector configuration, which is operating at a secondary weight flow ratio of 0.04, is presented in figure 15(b). The optimum spacing ratio for this ejector configuration was 0.3, and the flow field for this operating condition is presented in figure 20(b). Figure 20(d) shows the character of the primary flow field just below the spacing ratio where the secondary pressure peaks. It is evident from this plot that the expansion characteristics, and consequently the pumping action are controlled by the fact that the primary nozzle flow sees an ejector shroud which is basically convergent. The diverging section appears to have little influence over the initial ejector flow field.

Effect of Shroud Diameter Ratio for Cylindrical Ejectors

Ejector pumping characteristics are strongly influenced by the shroud diameter ratio D_S/D_p, as illustrated in figure 21. The calculations were performed on a family of cylindrical shroud ejectors having shroud diameter ratios of 1.41, 1.21, 1.11, and 1.06, all with an 8^o conical primary nozzle. The tabulated coordinates for this family of ejector nozzles are presented in tables VII to X. Results of the experimental investigations are presented in reference 10.

A comparison of the computed performance and the model data generally indicates good agreement except for the low-diameter-ratio ejector operating at high secondary mass flow rates. Under these conditions, the secondary inlet Mach number ranged from 0.3 to 0.6. In an attempt to account for the disagreement at this low diameter ratio, the secondary inlet flow blockage was increased by changing the initial shroud boundary layer displacement thickness δ^*/D_p from 0 to 0.0025. The results of this latter calculation are shown as the dashed line in figure 21 and indicate better agreement with data. Consequently, secondary boundary layer flow blockage can influence the pumping characteristics, particularly when the secondary inlet Mach number is high.

If the performances of the four ejector nozzles are examined in sequence at zero secondary weight flow ratio, it can be seen that agreement between predicted pumping and experimentally measured pumping became poorer as the shroud diameter ratio approached umity. However, agreement at 1 percent secondary weight flow ratio was very good. Computer flow field plots of this family of four ejector nozzles are presented in figure 22 for secondary weight flow ratios of 0 and 0.04. As the shroud diameter ratio was increased from 1.06 to 1.41, the impingement shock, which is clearly visible at zero secondary weight flow ratio, moved downstream and strengthened in the process due to the higher upstream Mach numbers. It should be emphasized that the shock was not of constant strength. As the shock wave approached the ejector centerline, its strength increased very rapidly depending on the initial expansion characteristics of the ejector nozzle. For the ejector nozzle having a shroud diameter ratio D_S/D_p of 1.41, the shock in the vicinity of the ejector centerline was sufficiently strong to cause subsonic conditions within the ejector flow field. This same phenomenon also occurred with this ejector nozzle at a secondary weight flow ratio of 0.04, except that a recompression region developed into a very strong shock wave which caused sonic flow within the nozzle.

The purpose of contouring the ejector shroud can therefore be viewed as an attempt to alleviate the strong recompression that follows the expansion processes in the vicinity of the primary nozzle lip. It is readily apparent therefore that the rationale for contouring an ejector nozzle shroud is fundamentally different from the reasons for shaping a convergent-divergent (C-D) nozzle. While the walls of the C-D nozzle are shaped to con-

trol the expansion process, the shroud of the ejector nozzle is contoured to control the recompression process. This fundamental difference can become very important in the design of ejector nozzles since a mismatch between the shroud contour and recompression flow field can result in large performance losses.

A major motivation for developing the procedures presented in reference 7 is to compute the performance of the conical primary nozzle which is typically used in ejector systems. Prediction of the flow and thrust coefficients from the analysis of reference 7 and the experimental data of reference 10 are compared in figure 23. These performance parameters are presented as a function of the nozzle pressure ratio. The flow coefficient is the ratio of actual to ideal mass flow W_p/W_{ip}, while the thrust coefficient is the ratio of the actual thrust to the ideal thrust of a choked nozzle based on the measured weight flow. Predictions of the flow coefficient in the lower nozzle pressure ratio range were approximately 0.7 percent below the measured values; however, very good agreement was achieved in the upper nozzle pressure ratio range. Since there is no apparent reason for the experimental flow coefficient to decrease as the pressure ratio was increased, it can be concluded that some measuring error occurred in the lower pressure ratio range. Because the nozzle thrust coefficient is based on the actual mass flow, the 0.7 percent disagreement in flow coefficient that existed in the low pressure ratio range was partly responsible for a 1.4 percent variation in the nozzle thrust coefficient. This sensitivity is a problem both in the measurement and prediction of ejector thrust performance and may explain the often contradictory ejector performances that have been reported.

As indicated in figure 7, the flow coefficient can vary substantially as a function of secondary weight flow ratio. The reason behind this occurrence lies in the fact that within an ejector system, the primary nozzle is sometimes forced to operate in the back pressure range, which includes the knee of the flow coefficient curve. This phenomenon must be taken into account in the practical design of ejector nozzles.

Effect of Primary Temperature

To investigate the ability to predict the performance of ejector nozzles at higher primary total temperatures, a series of solutions were obtained for the cylindrical shroud ejector whose test results are presented in reference 11. These ejector nozzles were tested with an afterburning turbojet engine mounted in an altitude facility. Power settings were varied from part power to maximum afterburning, yielding exhaust primary gas temperatures between 889 and 1945 K (1600° and 3500° R). In order to accommodate the flow, the primary nozzle angle was varied from 5° to 15°. Therefore, as the power setting was varied, both the nozzle lip angle and the shroud diameter ratio changed.

The secondary inlet temperature used in the calculations was based on the experimentally measured results. In general, the theory was able to predict fairly well both the pumping and thrust characteristics that were measured. The stream thrust (or vacuum thrust) parameter used to compare theory and data was defined in terms of the sonic throat area of the primary nozzle A_{p*} and the primary total pressure.

In an attempt to clarify the differences between "cold" and "hot" flow ejector nozzle testing, data from references 10 to 12 are compared in figure 24, along with some calculations. Three sets of data are presented for the cylindrical shroud ejector having a diameter ratio D_s/D_p of 1.11. The cold flow data presented in references 10 and 12 appear to form a reliable set since the measured pumping characteristics are essentially the same. When compared with the performance measured under the conditions when the primary temperature was about 1945 K (3500° R), both the data and calculations indicated that there was a decrease in pumping action. It is apparent for this ejector nozzle that the increase in thrust contribution from the larger secondary stream pressure did not compensate for the loss in thrust of the primary flow. Consequently, the effects of temperature on nozzle performance depend on geometric factors.

Plug Nozzle Ejectors

One type of ejector that has not received widespread analytical attention is the plug nozzle. It is pointed out in reference 13 that good performance can be achieved with a plug nozzle which incorporates a translating shroud and variable geometry primary nozzle. To investigate the question of effectiveness of this type of ejector nozzle, the "afterburning on" and "afterburning off" configurations discussed in reference 13 were calculated by using the current computer program and compared with measured performance. The results are presented in figures 25 and 26.

The analysis presented in reference 7 computed a primary nozzle inlet flow sonic line by assuming conical flow in the vicinity of the primary nozzle exit; that is, the primary inlet flow satisfies the Taylor-Maccoll equation. When the calculations were based on a primary nozzle whose exit area corresponds to the effective or sonic area A_{p*}, good agreement was achieved with the measured performance. As pointed out in reference 1, the assumption that the primary nozzle inlet flow satisfies the Taylor-Maccoll equation is equivalent to the plane sonic-line assumption previously discussed. This partially accounts for the fact that the computed efficiency tended to be higher than the measured efficiency.

The good theoretical results that were achieved are not inconsistent with the previous discussion on the sonic-line assumptions when it is realized that the difference

between lip angle and cone angle was less than 2° for the "afterburning on" configuration (fig. 25) and less than 7° for "afterburning off" configuration (fig. 26). As indicated in figure 10, the error due to the sonic-line assumptions was not very great in this range of primary nozzle lip angles.

CONCLUSIONS

The analysis described in NASA TN D-7602 provides an accurate and economical method of designing a wide variety of supersonic ejector nozzles over the range of flow conditions of interest. This conclusion was reached by comparisons with a substantial amount of ejector nozzle performance data. It was also concluded that the two-stream mixing process and the distribution of flow properties along the sonic line can have significant effect on both the thrust and pumping characteristics of ejector nozzles. These rather significant results indicate the necessity of accurately predicting the two-stream mixing process and the flow conditions in the transonic region of the primary nozzle and of including these effects in the hardware design.

In general, the initial expansion and recompression process dominates ejector nozzle performance. Therefore, those factors which affect this process strongly, such as the sonic line, the initial mixing process, the spacing ratio, the shroud shoulder diameter ratio, and so forth, are going to have the greatest influence on ejector performance. It was also concluded that the effect of primary temperature depends on such parameters as the shroud or shoulder diameter ratio and the spacing ratio. No a priori statement as to the merits of "cold" flow and "hot" flow testing can be made until these factors have been defined. The contouring of the shroud of ejector nozzles must take into account the initial expansion and recompression process if highly efficient nozzle performance is to be achieved.

Lewis Research Center,
National Aeronautics and Space Administration,
Cleveland, Ohio, September 19, 1973,
501-24.

REFERENCES

1. Anderson, B. H.: Factors Which Influence the Analysis and Design of Ejector Nozzles. Paper 72-46, AIAA, Jan. 1972.

2. Bernstein, A.; Heiser, W. H.; and Hevenor, C.: Compound-Compressible Nozzle Flow. J. Appl. Mech., vol. 34, no. 3, Sept. 1967, pp. 548-554.

3. Anon.: Users Manual for the General Ejector Nozzle Deck (Deck IV). Rep. PWA-3465, Suppl. A, Pratt & Whitney Aircraft, 1968.

4. Hardy, T. M.; and Lacombe, H.: Supersonic By-pass Nozzles - Computing Methods. Rev. Franc. de Mecanique, 4th Quarter, 1967, pp. 49-59.

5. Chow, W. L.; and Addy, A. L.: Interaction Between Primary and Secondary Streams of Supersonic Ejector Systems and Their Performance Characteristics. AIAA J., vol. 2, no. 4, Apr. 1964, pp. 686-695.

6. Beheim, Milton A.; Anderson, Bernhard H.; Clark, John S.; Corson, Blake W., Jr.; Stitt, Leonard E.; and Wilcox, Fred A.: Supersonic Exhaust Nozzles. Aircraft Propulsion. NASA SP-259, 1971, pp. 233-282,

7. Anderson, Bernhard H.: Computer Program for Calculating the Flow Field of Supersonic Ejector Nozzles. NASA TN D-7602, 1974.

8. Shrewsbury, George D.; and Jones, John R.: Static Performance of an Auxiliary Inlet Ejector Nozzle for Supersonic-Cruise Aircraft. NASA TM X-1653, 1968.

9. Lewis, W. G. E.; and Armstrong, F. W.: Some Experiments on Two-Stream Propelling Nozzles for Supersonic Aircraft. Paper 70-48, ICAS, Sept. 1970.

10. Greathouse, W. K.; and Hollister, D. P.: Air-Flow and Thrust Characteristics of Several Cylindrical Cooling-Air Ejectors With a Primary to Secondary Temperature Ratio of 1.0. NACA RM E52L24, 1953.

11. Samanich, N. E.; and Huntley, S. C.: Thrust and Pumping Characteristics of Cylindrical Ejectors Using Afterburning Turbojet Gas Generator. NASA TM X-52565, 1969.

12. Maphet, J. A.; and McKenzie, W. T.: Internal Performance of Several Cylindrical and Divergent Shroud Ejector Nozzles With Exit Diameter Ratios of 1.11, 1.19, 1.27. 1.35, 1.43, 1.53 and 1.65. Rep. FZA-4-341, General Dynamics/Convair, Dec. 1958.

13. Bresnahan, Donald L.: Experimental Investigation of a 10° Conical Turbojet Plug Nozzle With Iris Primary and Translating Shroud at Mach Numbers From 0 to 2.0. NASA TM X-1709, 1968.

TABLE I. - SHROUD COORDINATES FOR CONTOURED FLAP EJECTOR NOZZLE

WITH SHOULDER DIAMETER RATIO OF 1.370

Ratio of axial distance to radius of primary nozzle	Ratio of radial distance to radius of primary nozzle	Surface tangent	Surface angle, deg	Ratio of axial distance to radius of primary nozzle	Ratio of radial distance to radius of primary nozzle	Surface tangent	Surface angle, deg
-0.57531	2.09989	-0.00000	-0.00003	1.89723	1.54267	0.23903	13.44223
-0.52037	2.09989	0.00000	0.00004	1.95218	1.55586	0.24361	13.69124
-0.46542	2.09989	-0.00000	-0.00013	2.00712	1.56905	0.22652	12.76237
-0.41047	2.09989	0.00001	0.00047	2.06207	1.58062	0.20197	11.41820
-0.35553	2.09989	-0.00003	-0.00176	2.11702	1.59158	0.19560	11.06708
-0.30058	2.09989	0.00011	0.00657	2.17196	1.60205	0.18579	10.52502
-0.24564	2.09989	-0.00043	-0.02453	2.22691	1.61205	0.17930	10.16522
-0.19069	2.09989	0.00160	0.09155	2.28185	1.62185	0.17801	10.09372
-0.13575	2.09989	-0.00596	-0.34166	2.33680	1.63165	0.17884	10.13940
-0.08080	2.09989	0.02226	1.27491	2.39174	1.64154	0.18206	10.31820
-0.02586	2.09989	-0.08306	-4.74792	2.44669	1.65141	0.17160	9.73106
0.02909	2.08684	-0.40206	-21.90292	2.50163	1.66036	0.15915	9.04276
0.08403	2.05772	-0.61108	-31.42843	2.55658	1.66911	0.15821	8.99011
0.13898	2.02271	-0.65518	-33.23212	2.61152	1.67778	0.15865	9.01497
0.19393	1.98626	-0.66999	-33.82165	2.66647	1.68657	0.16034	9.10950
0.24887	1.94876	-0.70251	-35.08829	2.72142	1.69536	0.15997	9.08868
0.30382	1.90627	-0.88689	-41.56946	2.77636	1.70415	0.15977	9.07740
0.35876	1.85207	-1.02948	-45.83230	2.83131	1.71294	0.16095	9.14336
0.41371	1.79429	-1.10945	-47.97014	2.88625	1.72143	0.14019	7.98033
0.46865	1.72940	-1.23009	-50.89074	2.94120	1.72829	0.11654	6.64744
0.52360	1.66128	-1.23277	-50.95158	2.99614	1.73473	0.11970	6.82611
0.57854	1.59588	-1.12919	-48.47216	3.05109	1.74162	0.13214	7.52756
0.63349	1.53842	-0.95859	-43.78870	3.10603	1.74926	0.14479	8.23683
0.68843	1.49055	-0.78736	-38.21558	3.16098	1.75711	0.13441	7.65537
0.74338	1.45089	-0.67102	-33.86254	3.21592	1.76395	0.11959	6.81937
0.79832	1.41772	-0.50526	-26.80566	3.27087	1.77051	0.11916	6.79543
0.85327	1.39563	-0.32503	-18.00571	3.32582	1.77725	0.12988	7.40040
0.90822	1.38072	-0.21455	-12.10950	3.38076	1.78484	0.14337	8.15508
0.96316	1.37204	-0.10439	-5.95962	3.43571	1.79264	0.13696	7.79870
1.01811	1.36976	0.03383	1.93737	3.49065	1.79977	0.12398	7.06761
1.07305	1.37433	0.09400	5.37025	3.54560	1.80638	0.11759	6.70640
1.12800	1.37894	0.09098	5.19831	3.60054	1.81281	0.11794	6.72640
1.18294	1.38525	0.13816	7.86621	3.65549	1.81941	0.12174	6.94108
1.23789	1.39379	0.16759	9.51378	3.71043	1.82600	0.11510	6.56568
1.29283	1.40346	0.18564	10.51652	3.76538	1.83177	0.09298	5.31208
1.34778	1.41409	0.19798	11.19846	3.82032	1.83631	0.07584	4.33722
1.40272	1.42515	0.20664	11.67507	3.87527	1.84043	0.07623	4.35919
1.45767	1.43701	0.22699	12.78891	3.93022	1.84474	0.07991	4.56866
1.51262	1.45001	0.24276	13.64502	3.98516	1.84914	0.07998	4.57261
1.56756	1.46342	0.24400	13.71239	4.04011	1.85334	0.06928	3.96309
1.62251	1.47674	0.24084	13.54131	4.09505	1.85675	0.05857	3.35215
1.67745	1.48993	0.23977	13.48328	4.15000	1.85996	0.05811	3.32599
1.73240	1.50311	0.24008	13.50000	4.20494	1.86317	0.05918	3.38698
1.78734	1.51630	0.23991	13.49109	4.25989	1.86646	0.06026	3.44821
1.84229	1.52949	0.24026	13.51001	4.31483	1.86976	0.05980	3.42197

TABLE II. - SHROUD COORDINATES FOR CONICAL FLAP EJECTOR NOZZLE

WITH SHOULDER DIAMETER RATIO OF 1.183

Ratio of axial distance to radius of primary nozzle	Ratio of radial distance to radius of primary nozzle	Surface tangent	Surface angle, deg	Ratio of axial distance to radius of primary nozzle	Ratio of radial distance to radius of primary nozzle	Surface tangent	Surface angle, deg
-1.60530	1.65800	-0.00000	-0.00000	1.30697	1.20705	0.15528	8.82617
-1.54058	1.65800	0.00000	0.00000	1.37169	1.21722	0.15826	8.95297
-1.47587	1.65800	-0.00000	-0.00000	1.43640	1.22748	0.15866	9.01546
-1.41115	1.65800	0.00000	0.00000	1.50112	1.23774	0.15860	9.01205
-1.34643	1.65800	-0.00000	-0.00000	1.56584	1.24801	0.15866	9.01513
-1.28171	1.65800	0.00000	0.00000	1.63055	1.25827	0.15844	9.00317
-1.21700	1.65800	-0.00000	-0.00000	1.69527	1.26852	0.15863	9.01386
-1.15228	1.65800	0.00000	0.00000	1.75999	1.27878	0.15793	8.97460
-1.08756	1.65800	-0.00000	-0.00000	1.82471	1.28897	0.15758	8.95527
-1.02285	1.65800	0.00000	0.00000	1.88942	1.29921	0.15859	9.01168
-0.95813	1.65800	-0.00000	-0.00000	1.95414	1.30948	0.15867	9.01585
-0.89341	1.65800	0.00000	0.00000	2.01886	1.31974	0.15859	9.01135
-0.82870	1.65800	-0.00000	-0.00000	2.08357	1.33001	0.15864	9.01448
-0.76398	1.65800	0.00000	0.00000	2.14829	1.34027	0.15850	9.00644
-0.69926	1.65800	-0.00000	-0.00000	2.21301	1.35053	0.15856	9.00982
-0.63454	1.65800	0.00000	0.00000	2.27772	1.36079	0.15815	8.98663
-0.56983	1.65800	-0.00000	-0.00000	2.34244	1.37099	0.15758	8.95483
-0.50511	1.65800	0.00000	0.00000	2.40716	1.38121	0.15834	8.99758
-0.44039	1.65800	-0.00000	-0.00000	2.47188	1.39148	0.15875	9.02063
-0.37568	1.65800	0.00000	0.00000	2.53659	1.40175	0.15858	9.01106
-0.31096	1.65800	-0.00000	-0.00000	2.60131	1.41201	0.15858	9.01090
-0.24624	1.65800	0.00000	0.00000	2.66603	1.42227	0.15843	9.00228
-0.18152	1.65800	-0.00000	-0.00000	2.73074	1.43252	0.15860	9.01206
-0.11681	1.65800	0.00000	0.00000	2.79546	1.44279	0.15844	9.00295
-0.05209	1.65800	-0.00000	-0.00001	2.86018	1.45302	0.15755	8.95316
0.01263	1.65800	0.00000	0.00002	2.92490	1.46321	0.15812	8.98512
0.07734	1.65800	-0.00000	-0.00009	2.98961	1.47348	0.15882	9.02419
0.14206	1.65800	0.00001	0.00032	3.05433	1.48375	0.15856	9.00970
0.20678	1.65800	-0.00002	-0.00118	3.11905	1.49401	0.15861	9.01281
0.27150	1.65800	0.00008	0.00442	3.18376	1.50427	0.15844	9.00311
0.33621	1.65800	-0.00029	-0.01649	3.24848	1.51453	0.15851	9.00711
0.40093	1.65800	0.00107	0.06156	3.31320	1.52479	0.15865	9.01479
0.46565	1.65800	-0.00401	-0.22973	3.37791	1.53504	0.15756	8.95404
0.53036	1.65226	-0.25109	-14.09520	3.44263	1.54522	0.15791	8.97354
0.59508	1.61899	-0.79996	-38.65832	3.50735	1.55549	0.15885	9.02613
0.65980	1.55538	-1.03993	-46.12131	3.57207	1.56575	0.15856	9.00981
0.72451	1.49066	-0.98903	-44.68406	3.63678	1.57601	0.15846	9.00436
0.78923	1.42594	-1.00441	-45.12602	3.70150	1.58626	0.15849	9.00600
0.85395	1.36122	-0.99367	-44.81795	3.76622	1.59653	0.15860	9.01226
0.91867	1.29650	-1.02093	-45.59338	3.83093	1.60680	0.15878	9.02206
0.98338	1.23480	-0.78272	-38.05092	3.89565	1.61705	0.15761	8.95692
1.04810	1.19893	-0.37135	-20.37271	3.96037	1.62722	0.15772	8.96268
1.11282	1.18409	-0.08259	-4.72129	4.02509	1.63749	0.15887	9.02730
1.17753	1.18650	0.12574	7.16651	4.08980	1.64775	0.15853	9.00803
1.24225	1.19678	0.16783	9.52692	4.15452	1.65802	0.15868	9.01628

TABLE III. - SHROUD COORDINATES FOR CONICAL FLAP EJECTOR NOZZLE

WITH SHOULDER DIAMETER RATIO OF 1.225

Ratio of axial distance to radius of primary nozzle	Ratio of radial distance to radius of primary nozzle	Surface tangent	Surface angle, deg	Ratio of axial distance to radius of primary nozzle	Ratio of radial distance to radius of primary nozzle	Surface tangent	Surface angle, deg
-1.48240	1.65800	-0.00000	-0.00000	1.36773	1.22724	-0.12753	-7.26777
-1.41906	1.65800	0.00000	0.00000	1.43106	1.22688	0.09942	5.67794
-1.35573	1.65800	-0.00000	-0.00000	1.49440	1.23655	0.17103	9.70538
-1.29239	1.65800	0.00000	0.00000	1.55774	1.24673	0.15680	8.91142
-1.22906	1.65800	-0.00000	-0.00000	1.62107	1.25676	0.15865	9.01482
-1.16572	1.65800	0.00000	0.00000	1.68441	1.26678	0.15839	9.00041
-1.10238	1.65800	-0.00000	-0.00000	1.74775	1.27683	0.15837	8.99922
-1.03905	1.65800	0.00000	0.00000	1.81108	1.28685	0.15852	9.00780
-0.97571	1.65800	-0.00000	-0.00000	1.87442	1.29690	0.15816	8.98757
-0.91237	1.65800	0.00000	0.00000	1.93775	1.30690	0.15863	9.01376
-0.84904	1.65800	-0.00000	-0.00000	2.00109	1.31697	0.15829	8.99482
-0.78570	1.65800	0.00000	0.00000	2.06443	1.32697	0.15855	9.00916
-0.72237	1.65800	-0.00000	-0.00000	2.12776	1.33705	0.15840	9.00075
-0.65903	1.65800	0.00000	0.00000	2.19110	1.34703	0.15822	8.99061
-0.59569	1.65800	-0.00000	-0.00000	2.25443	1.35710	0.15856	9.00997
-0.53236	1.65800	0.00000	0.00000	2.31777	1.36710	0.15829	8.99467
-0.46902	1.65800	-0.00000	-0.00000	2.38111	1.37717	0.15879	9.02256
-0.40568	1.65800	0.00000	0.00000	2.44444	1.38718	0.15755	8.95324
-0.34235	1.65800	-0.00000	-0.00000	2.50778	1.39716	0.15805	8.98144
-0.27901	1.65800	0.00000	0.00000	2.57112	1.40720	0.15864	9.01418
-0.21568	1.65800	-0.00000	-0.00000	2.63445	1.41724	0.15829	8.99477
-0.15234	1.65800	0.00000	0.00000	2.69779	1.42727	0.15857	9.01063
-0.08900	1.65800	-0.00000	-0.00000	2.76112	1.43731	0.15831	8.99893
-0.02567	1.65800	0.00000	0.00000	2.82446	1.44733	0.15855	9.00916
0.03767	1.65800	-0.00000	-0.00000	2.88780	1.45738	0.15815	8.98699
0.10100	1.65800	0.00000	0.00000	2.95113	1.46738	0.15863	9.01351
0.16434	1.65800	-0.00000	-0.00000	3.01447	1.47746	0.15829	8.99487
0.22768	1.65800	0.00000	0.00002	3.07780	1.48745	0.15857	9.01056
0.29101	1.65800	-0.00000	-0.00007	3.14114	1.49753	0.15827	8.99374
0.35435	1.65800	0.00000	0.00025	3.20448	1.50750	0.15817	8.98829
0.41769	1.65800	-0.00002	-0.00093	3.26781	1.51758	0.15880	9.02312
0.48102	1.65800	0.00006	0.00349	3.33115	1.52759	0.15822	8.99056
0.54436	1.65800	-0.00023	-0.01302	3.39449	1.53765	0.15862	9.01296
0.60769	1.65800	0.00085	0.04858	3.45782	1.54767	0.15829	8.99482
0.67103	1.65800	-0.00316	-0.18130	3.52116	1.55771	0.15851	9.00729
0.73437	1.65800	0.01181	0.67661	3.58449	1.56773	0.15818	8.98861
0.79770	1.65786	-0.05070	-2.90213	3.64783	1.57776	0.15865	9.01505
0.86104	1.64420	-0.46259	-24.82459	3.71117	1.58781	0.15825	8.99275
0.92437	1.59817	-0.92622	-42.80639	3.77450	1.59783	0.15860	9.01215
0.98771	1.53465	-1.02143	-45.60728	3.83784	1.60789	0.15829	8.99487
1.05105	1.47132	-0.99667	-44.90447	3.90118	1.61789	0.15838	8.99993
1.11438	1.40792	-0.99498	-44.85570	3.96451	1.62795	0.15842	9.00214
1.17772	1.34458	-1.02648	-45.74866	4.02785	1.63795	0.15840	9.00103
1.24106	1.28282	-0.82436	-39.50066	4.09118	1.64802	0.15876	9.02106
1.30439	1.24442	-0.42021	-22.79256	4.15452	1.65802	0.15703	8.92403

TABLE IV. - SHROUD COORDINATES FOR CONICAL FLAP EJECTOR NOZZLE

WITH SHOULDER DIAMETER RATIO OF 1.265

Ratio of axial distance to radius of primary nozzle	Ratio of radial distance to radius of primary nozzle	Surface tangent	Surface angle, deg	Ratio of axial distance to radius of primary nozzle	Ratio of radial distance to radius of primary nozzle	Surface tangent	Surface angle, deg
-1.36540	1.65800	-0.00000	-0.00000	1.42557	1.38933	-1.02932	-45.82769
-1.30338	1.65800	0.00000	0.00000	1.48759	1.32801	-0.85621	-40.57037
-1.24136	1.65800	-0.00000	-0.00000	1.54961	1.28765	-0.46400	-24.89119
-1.17934	1.65800	0.00000	0.00000	1.61164	1.26851	-0.16570	-9.40827
-1.11731	1.65800	-0.00000	-0.00000	1.67366	1.26589	0.07396	4.23003
-1.05529	1.65800	0.00000	0.00000	1.73568	1.27471	0.16985	9.63990
-0.99327	1.65800	-0.00000	-0.00000	1.79770	1.28473	0.15815	8.98679
-0.93125	1.65800	0.00000	0.00000	1.85972	1.29458	0.15849	9.00614
-0.86923	1.65800	-0.00000	-0.00000	1.92174	1.30436	0.15756	8.95379
-0.80721	1.65800	0.00000	0.00000	1.98376	1.31417	0.15885	9.02617
-0.74518	1.65800	-0.00000	-0.00000	2.04579	1.32404	0.15849	9.00611
-0.68316	1.65800	0.00000	0.00000	2.10781	1.33383	0.15826	8.99278
-0.62114	1.65800	-0.00000	-0.00000	2.16983	1.34368	0.15886	9.02639
-0.55912	1.65800	0.00000	0.00000	2.23185	1.35350	0.15790	8.97276
-0.49710	1.65800	-0.00000	-0.00000	2.29387	1.36329	0.15797	8.97703
-0.43508	1.65800	0.00000	0.00000	2.35589	1.37311	0.15886	9.02632
-0.37305	1.65800	-0.00000	-0.00000	2.41792	1.38296	0.15826	8.99327
-0.31103	1.65800	0.00000	0.00000	2.47994	1.39277	0.15877	9.02182
-0.24901	1.65800	-0.00000	-0.00000	2.54196	1.40265	0.15867	9.01570
-0.18699	1.65800	0.00000	0.00000	2.60398	1.41243	0.15735	8.94205
-0.12497	1.65800	-0.00000	-0.00000	2.66600	1.42222	0.15848	9.00540
-0.06295	1.65800	0.00000	0.00000	2.72802	1.43207	0.15874	9.01961
-0.00093	1.65800	-0.00000	-0.00000	2.79005	1.44189	0.15829	8.99464
0.06110	1.65800	0.00000	0.00000	2.85207	1.45172	0.15886	9.02683
0.12312	1.65800	-0.00000	-0.00000	2.91409	1.46157	0.15826	8.99313
0.18514	1.65800	0.00000	0.00000	2.97611	1.47135	0.15745	8.94800
0.24716	1.65800	-0.00000	-0.00000	3.03813	1.48115	0.15889	9.02846
0.30918	1.65800	0.00000	0.00000	3.10015	1.49102	0.15846	9.00416
0.37120	1.65800	-0.00000	-0.00000	3.16217	1.50081	0.15840	9.00068
0.43323	1.65800	0.00000	0.00000	3.22420	1.51068	0.15885	9.02614
0.49525	1.65800	-0.00000	-0.00000	3.28622	1.52049	0.15812	8.98515
0.55727	1.65800	0.00000	0.00001	3.34824	1.53032	0.15883	9.02496
0.61929	1.65800	-0.00000	-0.00005	3.41026	1.54017	0.15820	8.98596
0.68131	1.65800	0.00000	0.00018	3.47228	1.54994	0.15750	8.95030
0.74333	1.65800	-0.00001	-0.00065	3.53430	1.55975	0.15910	9.04019
0.80535	1.65800	0.00004	0.00244	3.59633	1.56963	0.15837	8.99931
0.86738	1.65800	-0.00016	-0.00910	3.65835	1.57941	0.15826	8.99277
0.92940	1.65800	0.00059	0.03396	3.72037	1.58928	0.15899	9.03369
0.99142	1.65800	-0.00221	-0.12673	3.78239	1.59909	0.15764	8.95824
1.05344	1.65800	0.00825	0.47294	3.84441	1.60887	0.15805	8.98123
1.11546	1.65547	-0.15325	-8.71292	3.90643	1.61870	0.15902	9.03544
1.17748	1.63149	-0.67775	-34.12761	3.96846	1.62856	0.15818	8.98865
1.23951	1.57539	-1.00896	-45.25560	4.03048	1.63835	0.15860	9.01216
1.30153	1.51337	-0.99956	-44.98753	4.09250	1.64823	0.15893	9.03048
1.36355	1.45135	-0.99278	-44.79240	4.15452	1.65802	0.15699	8.92214

TABLE V. - SHROUD COORDINATES FOR CONICAL FLAP EJECTOR NOZZLE

WITH SHOULDER DIAMETER RATIO OF 1.304

Ratio of axial distance to radius of primary nozzle	Ratio of radial distance to radius of primary nozzle	Surface tangent	Surface angle, deg	Ratio of axial distance to radius of primary nozzle	Ratio of radial distance to radius of primary nozzle	Surface tangent	Surface angle, deg
-1.25130	1.65800	0.00000	0.00000	1.48198	1.61740	-0.81783	-39.27729
-1.19056	1.65800	-0.00000	-0.00000	1.54272	1.55738	-1.04097	-46.14988
-1.12982	1.65800	0.00000	0.00000	1.60346	1.49664	-0.98265	-44.49862
-1.06908	1.65800	-0.00000	-0.00000	1.66420	1.43590	-1.02844	-45.80316
-1.00834	1.65800	0.00000	0.00000	1.72494	1.37527	-0.89835	-41.93503
-0.94760	1.65800	-0.00000	-0.00000	1.78568	1.33158	-0.53090	-27.96397
-0.88686	1.65800	0.00000	0.00000	1.84642	1.30974	-0.21433	-12.09702
-0.82612	1.65800	-0.00000	-0.00000	1.90716	1.30417	0.03451	1.97665
-0.76538	1.65800	0.00000	0.00000	1.96790	1.31151	0.16327	9.27277
-0.70464	1.65800	-0.00000	-0.00000	2.02864	1.32133	0.15982	9.08612
-0.64390	1.65800	0.00000	0.00000	2.08938	1.33096	0.15808	8.98295
-0.58316	1.65800	-0.00000	-0.00000	2.15011	1.34057	0.15847	9.00452
-0.52243	1.65800	0.00000	0.00000	2.21085	1.35020	0.15848	9.00512
-0.46169	1.65800	-0.00000	-0.00000	2.27159	1.35982	0.15837	8.99922
-0.40095	1.65800	0.00000	0.00000	2.33233	1.36944	0.15848	9.00522
-0.34021	1.65800	-0.00000	-0.00000	2.39307	1.37907	0.15841	9.00132
-0.27947	1.65800	0.00000	0.00000	2.45381	1.38869	0.15840	9.00062
-0.21873	1.65800	-0.00000	-0.00000	2.51455	1.39831	0.15851	9.00692
-0.15799	1.65800	0.00000	0.00000	2.57529	1.40793	0.15833	8.99679
-0.09725	1.65800	-0.00000	-0.00000	2.63603	1.41755	0.15831	8.99571
-0.03651	1.65800	0.00000	0.00000	2.69677	1.42715	0.15744	8.94713
0.02423	1.65800	-0.00000	-0.00000	2.75751	1.43670	0.15763	8.95792
0.08497	1.65800	0.00000	0.00000	2.81825	1.44631	0.15861	9.01271
0.14571	1.65800	-0.00000	-0.00000	2.87899	1.45594	0.15847	9.00464
0.20645	1.65800	0.00000	0.00000	2.93973	1.46557	0.15837	8.99917
0.26719	1.65800	-0.00000	-0.00000	3.00047	1.47519	0.15848	9.00550
0.32793	1.65800	0.00000	0.00000	3.06121	1.48481	0.15840	9.00067
0.38867	1.65800	-0.00000	-0.00000	3.12195	1.49443	0.15841	9.00148
0.44941	1.65800	0.00000	0.00000	3.18269	1.50406	0.15849	9.00613
0.51015	1.65800	-0.00000	-0.00000	3.24343	1.51368	0.15836	8.99853
0.57089	1.65800	0.00000	0.00000	3.30417	1.52330	0.15849	9.00572
0.63163	1.65800	-0.00000	-0.00000	3.36491	1.53293	0.15841	9.00136
0.69237	1.65800	0.00000	0.00000	3.42565	1.54254	0.15826	8.99309
0.75311	1.65800	-0.00000	-0.00000	3.48638	1.55216	0.15844	9.00303
0.81384	1.65800	0.00000	0.00001	3.54712	1.56179	0.15849	9.00592
0.87458	1.65800	-0.00000	-0.00003	3.60786	1.57141	0.15836	8.99871
0.93532	1.65800	0.00000	0.00011	3.66860	1.58103	0.15849	9.00579
0.99606	1.65800	-0.00001	-0.00042	3.72934	1.59066	0.15839	9.00025
1.05680	1.65800	0.00003	0.00156	3.79008	1.60027	0.15842	9.00226
1.11754	1.65800	-0.00010	-0.00582	3.85082	1.60990	0.15848	9.00552
1.17828	1.65800	0.00038	0.02171	3.91156	1.61952	0.15836	8.99850
1.23902	1.65800	-0.00141	-0.08102	3.97230	1.62915	0.15849	9.00607
1.29976	1.65800	0.00528	0.30238	4.03304	1.63877	0.15839	9.00029
1.36050	1.65800	-0.01970	-1.12835	4.09378	1.64839	0.15841	9.00118
1.42124	1.65060	-0.29196	-16.27573	4.15452	1.65802	0.15866	9.01532

TABLE VI. - SHROUD COORDINATES FOR CONICAL FLAP EJECTOR NOZZLE

WITH SHOULDER DIAMETER RATIO OF 1.342

Ratio of axial distance to radius of primary nozzle	Ratio of radial distance to radius of primary nozzle	Surface tangent	Surface angle, deg	Ratio of axial distance to radius of primary nozzle	Ratio of radial distance to radius of primary nozzle	Surface tangent	Surface angle, deg
-1.14010	1.65800	0.00000	0.00000	1.53696	1.65800	-0.00335	-0.19176
-1.08061	1.65800	-0.00000	-0.00000	1.59645	1.65800	0.01249	0.71564
-1.02112	1.65800	0.00000	0.00000	1.65594	1.65777	-0.05839	-3.34194
-0.96163	1.65800	-0.00000	-0.00000	1.71543	1.64478	-0.44557	-24.01637
-0.90214	1.65800	0.00000	0.00000	1.77492	1.60327	-0.90738	-42.21984
-0.84265	1.65800	-0.00000	-0.00000	1.83441	1.54369	-1.02253	-45.63833
-0.78316	1.65800	0.00000	0.00000	1.89390	1.48420	-1.00692	-45.19761
-0.72367	1.65800	-0.00000	-0.00000	1.95339	1.42471	-0.94978	-43.52458
-0.66418	1.65800	0.00000	0.00000	2.01288	1.37660	-0.62013	-31.80434
-0.60469	1.65800	-0.00000	-0.00000	2.07237	1.35126	-0.27391	-15.31833
-0.54520	1.65800	0.00000	0.00000	2.13186	1.34215	-0.02167	-1.24113
-0.48571	1.65800	-0.00000	-0.00000	2.19135	1.34698	0.14466	8.23121
-0.42622	1.65800	0.00000	0.00000	2.25084	1.35643	0.16305	9.26061
-0.36673	1.65800	-0.00000	-0.00000	2.31033	1.36591	0.15788	8.97158
-0.30724	1.65800	0.00000	0.00000	2.36982	1.37532	0.15838	8.99967
-0.24775	1.65800	-0.00000	-0.00000	2.42931	1.38473	0.15791	8.97364
-0.18826	1.65800	0.00000	0.00000	2.48880	1.39414	0.15861	9.01288
-0.12877	1.65800	-0.00000	-0.00000	2.54829	1.40361	0.15939	9.05637
-0.06928	1.65800	0.00000	0.00000	2.60778	1.41307	0.15846	9.00400
-0.00979	1.65800	-0.00000	-0.00000	2.66727	1.42247	0.15810	8.98436
0.04970	1.65800	0.00000	0.00000	2.72676	1.43189	0.15818	8.98874
0.10919	1.65800	-0.00000	-0.00000	2.78625	1.44129	0.15802	8.97988
0.16868	1.65800	0.00000	0.00000	2.84574	1.45070	0.15824	8.99186
0.22817	1.65800	-0.00000	-0.00000	2.90523	1.46011	0.15810	8.98383
0.28766	1.65800	0.00000	0.00000	2.96472	1.46952	0.15880	9.02205
0.34715	1.65800	-0.00000	-0.00000	3.02421	1.47900	0.15934	9.05356
0.40664	1.65800	0.00000	0.00000	3.08370	1.48845	0.15824	8.99217
0.46613	1.65800	-0.00000	-0.00000	3.14319	1.49784	0.15800	8.97858
0.52562	1.65800	0.00000	0.00000	3.20268	1.50726	0.15831	8.99578
0.58511	1.65800	-0.00000	-0.00000	3.26217	1.51667	0.15816	8.98758
0.64460	1.65800	0.00000	0.00000	3.32166	1.52608	0.15810	8.98399
0.70409	1.65800	-0.00000	-0.00000	3.38115	1.53548	0.15798	8.97749
0.76358	1.65800	0.00000	0.00000	3.44064	1.54489	0.15886	9.02641
0.82307	1.65800	-0.00000	-0.00000	3.50013	1.55437	0.15937	9.05507
0.88256	1.65800	0.00000	0.00000	3.55962	1.56383	0.15839	9.00053
0.94205	1.65800	-0.00000	-0.00000	3.61911	1.57323	0.15794	8.97512
1.00154	1.65800	0.00000	0.00000	3.67860	1.58263	0.15813	8.98552
1.06103	1.65800	-0.00000	-0.00001	3.73809	1.59204	0.15823	8.99163
1.12052	1.65800	0.00000	0.00002	3.79758	1.60146	0.15828	8.99422
1.18001	1.65800	-0.00000	-0.00007	3.85707	1.61087	0.15789	8.97200
1.23950	1.65800	0.00000	0.00026	3.91656	1.62027	0.15872	9.01883
1.29899	1.65800	-0.00002	-0.00099	3.97605	1.62975	0.15941	9.05719
1.35848	1.65800	0.00006	0.00369	4.03554	1.63920	0.15836	8.99879
1.41797	1.65800	-0.00024	-0.01377	4.09503	1.64861	0.15809	8.98341
1.47746	1.65800	0.00090	0.05138	4.15452	1.65802	0.15834	8.99753

TABLE VII. - SHROUD COORDINATES FOR CYLINDRICAL SHROUD EJECTOR NOZZLE

WITH SHROUD DIAMETER RATIO OF 1.41

Ratio of axial distance to radius of primary nozzle	Ratio of radial distance to radius of primary nozzle	Surface tangent	Surface angle, deg	Ratio of axial distance to radius of primary nozzle	Ratio of radial distance to radius of primary nozzle	Surface tangent	Surface angle, deg
-1.40364	1.66243	-0.14055	-8.00038	0.53978	1.41000	0.00047	0.02718
-1.36045	1.65636	-0.14054	-8.00018	0.58296	1.41000	-0.00013	-0.00728
-1.31726	1.65029	-0.14054	-7.99971	0.62615	1.41000	0.00003	0.00195
-1.27408	1.64422	-0.14053	-7.99959	0.66934	1.41000	-0.00001	-0.00052
-1.23089	1.63816	-0.14054	-8.00015	0.71252	1.41000	0.00000	0.00014
-1.18770	1.63209	-0.14055	-8.00035	0.75571	1.41000	-0.00000	-0.00004
-1.14451	1.62602	-0.14054	-8.00021	0.79890	1.41000	0.00000	0.00001
-1.10133	1.61995	-0.14054	-7.99985	0.84208	1.41000	-0.00000	-0.00000
-1.05814	1.61388	-0.14053	-7.99953	0.88527	1.41000	0.00000	0.00000
-1.01495	1.60781	-0.14054	-7.99996	0.92846	1.41000	-0.00000	-0.00000
-0.97177	1.60174	-0.14055	-8.00029	0.97164	1.41000	0.00000	0.00000
-0.92858	1.59567	-0.14055	-8.00040	1.01483	1.41000	-0.00000	-0.00000
-0.88539	1.58960	-0.14054	-7.99994	1.05802	1.41000	0.00000	0.00000
-0.84221	1.58353	-0.14053	-7.99934	1.10121	1.41000	-0.00000	-0.00000
-0.79902	1.57746	-0.14054	-7.99992	1.14439	1.41000	0.00000	0.00000
-0.75583	1.57139	-0.14055	-8.00040	1.18758	1.41000	-0.00000	-0.00000
-0.71265	1.56532	-0.14055	-8.00028	1.23077	1.41000	0.00000	0.00000
-0.66946	1.55925	-0.14054	-7.99999	1.27395	1.41000	-0.00000	-0.00000
-0.62627	1.55318	-0.14053	-7.99948	1.31714	1.41000	0.00000	0.00000
-0.58308	1.54711	-0.14054	-7.99987	1.36033	1.41000	-0.00000	-0.00000
-0.53990	1.54104	-0.14055	-8.00040	1.40351	1.41000	0.00000	0.00000
-0.49671	1.53497	-0.14055	-8.00029	1.44670	1.41000	-0.00000	-0.00000
-0.45352	1.52890	-0.14054	-8.00004	1.48989	1.41000	0.00000	0.00000
-0.41034	1.52283	-0.14053	-7.99952	1.53307	1.41000	-0.00000	-0.00000
-0.36715	1.51676	-0.14054	-7.99975	1.57626	1.41000	0.00000	0.00000
-0.32396	1.51070	-0.14055	-8.00028	1.61945	1.41000	-0.00000	-0.00000
-0.28078	1.50463	-0.14055	-8.00032	1.66264	1.41000	0.00000	0.00000
-0.23759	1.49856	-0.14054	-8.00020	1.70582	1.41000	-0.00000	-0.00000
-0.19440	1.49249	-0.14053	-7.99953	1.74901	1.41000	0.00000	0.00000
-0.15122	1.48642	-0.14053	-7.99959	1.79220	1.41000	-0.00000	-0.00000
-0.10803	1.48035	-0.14055	-8.00033	1.83538	1.41000	0.00000	0.00000
-0.06484	1.47428	-0.14055	-8.00032	1.87857	1.41000	-0.00000	-0.00000
-0.02165	1.46821	-0.14054	-8.00013	1.92176	1.41000	0.00000	0.00000
0.02153	1.46214	-0.14054	-7.99968	1.96494	1.41000	-0.00000	-0.00000
0.06472	1.45607	-0.14054	-7.99972	2.00813	1.41000	0.00000	0.00000
0.10791	1.45000	-0.14054	-7.99989	2.05132	1.41000	-0.00000	-0.00000
0.15109	1.44393	-0.14057	-8.00168	2.09450	1.41000	0.00000	0.00000
0.19428	1.43786	-0.14045	-7.99509	2.13769	1.41000	-0.00000	-0.00000
0.23747	1.43179	-0.14087	-8.01876	2.18088	1.41000	0.00000	0.00000
0.28065	1.42572	-0.13927	-7.92880	2.22407	1.41000	-0.00000	-0.00000
0.32384	1.41965	-0.14524	-8.26377	2.26725	1.41000	0.00000	0.00000
0.36703	1.41358	-0.12302	-7.01307	2.31044	1.41000	-0.00000	-0.00000
0.41021	1.41000	-0.03317	-1.89998	2.35363	1.41000	0.00000	0.00000
0.45340	1.41004	0.00944	0.54112	2.39681	1.41000	-0.00000	-0.00000
0.49659	1.41002	-0.00306	-0.17534	2.44000	1.41000	0.00000	0.00000

TABLE VIII. - SHROUD COORDINATES FOR CYLINDRICAL SHROUD EJECTOR NOZZLE

WITH SHROUD DIAMETER RATIO OF 1.06

Ratio of axial distance to radius of primary nozzle	Ratio of radial distance to radius of primary nozzle	Surface tangent	Surface angle, deg	Ratio of axial distance to radius of primary nozzle	Ratio of radial distance to radius of primary nozzle	Surface tangent	Surface angle, deg
-1.60364	1.46243	-0.14055	-8.00051	0.42067	1.21000	0.00002	0.00111
-1.55865	1.45611	-0.14055	-8.00026	0.46566	1.21000	-0.00001	-0.00030
-1.51367	1.44979	-0.14053	-7.99961	0.51064	1.21000	0.00000	0.00008
-1.46868	1.44347	-0.14053	-7.99952	0.55563	1.21000	-0.00000	-0.00002
-1.42370	1.43714	-0.14055	-8.00024	0.60061	1.21000	0.00000	0.00001
-1.37871	1.43082	-0.14055	-8.00036	0.64560	1.21000	-0.00000	-0.00000
-1.33373	1.42450	-0.14054	-8.00011	0.69058	1.21000	0.00000	0.00000
-1.28874	1.41818	-0.14054	-7.99969	0.73557	1.21000	-0.00000	-0.00000
-1.24376	1.41186	-0.14053	-7.99963	0.78055	1.21000	0.00000	0.00000
-1.19877	1.40553	-0.14054	-8.00016	0.82554	1.21000	-0.00000	-0.00000
-1.15379	1.39921	-0.14055	-8.00033	0.87052	1.21000	0.00000	0.00000
-1.10880	1.39289	-0.14054	-8.00023	0.91551	1.21000	-0.00000	-0.00000
-1.06382	1.38657	-0.14053	-7.99957	0.96049	1.21000	0.00000	0.00000
-1.01884	1.38024	-0.14053	-7.99958	1.00548	1.21000	-0.00000	-0.00000
-0.97385	1.37392	-0.14055	-8.00032	1.05046	1.21000	0.00000	0.00000
-0.92887	1.36760	-0.14055	-8.00033	1.09544	1.21000	-0.00000	-0.00000
-0.88388	1.36128	-0.14054	-8.00009	1.14043	1.21000	0.00000	0.00000
-0.83890	1.35496	-0.14053	-7.99960	1.18541	1.21000	-0.00000	-0.00000
-0.79391	1.34863	-0.14054	-7.99974	1.23040	1.21000	0.00000	0.00000
-0.74893	1.34231	-0.14055	-8.00034	1.27538	1.21000	-0.00000	-0.00000
-0.70394	1.33599	-0.14055	-8.00031	1.32037	1.21000	0.00000	0.00000
-0.65896	1.32967	-0.14054	-8.00009	1.36535	1.21000	-0.00000	-0.00000
-0.61397	1.32334	-0.14053	-7.99956	1.41034	1.21000	0.00000	0.00000
-0.56899	1.31702	-0.14054	-7.99971	1.45532	1.21000	-0.00000	-0.00000
-0.52400	1.31070	-0.14055	-8.00027	1.50031	1.21000	0.00000	0.00000
-0.47902	1.30438	-0.14055	-8.00032	1.54529	1.21000	-0.00000	-0.00000
-0.43403	1.29806	-0.14054	-8.00016	1.59028	1.21000	0.00000	0.00000
-0.38905	1.29173	-0.14053	-7.99943	1.63526	1.21000	-0.00000	-0.00000
-0.34407	1.28541	-0.14054	-7.99972	1.68025	1.21000	0.00000	0.00000
-0.29908	1.27909	-0.14055	-8.00042	1.72523	1.21000	-0.00000	-0.00000
-0.25410	1.27277	-0.14055	-8.00028	1.77021	1.21000	0.00000	0.00000
-0.20911	1.26645	-0.14054	-8.00006	1.81520	1.21000	-0.00000	-0.00000
-0.16413	1.26012	-0.14053	-7.99947	1.86018	1.21000	0.00000	0.00000
-0.11914	1.25380	-0.14054	-7.99994	1.90517	1.21000	-0.00000	-0.00000
-0.07416	1.24748	-0.14054	-8.00001	1.95015	1.21000	0.00000	0.00000
-0.02917	1.24116	-0.14057	-8.00181	1.99514	1.21000	-0.00000	-0.00000
0.01581	1.23483	-0.14044	-7.99431	2.04012	1.21000	0.00000	0.00000
0.06080	1.22851	-0.14091	-8.02077	2.08511	1.21000	-0.00000	-0.00000
0.10578	1.22219	-0.13913	-7.92046	2.13009	1.21000	0.00000	0.00000
0.15077	1.21587	-0.14582	-8.29617	2.17508	1.21000	-0.00000	-0.00000
0.19575	1.21041	-0.06345	-3.63038	2.22006	1.21000	0.00000	0.00000
0.24074	1.21003	0.01048	0.60046	2.26505	1.21000	-0.00000	-0.00000
0.28572	1.21004	-0.00317	-0.18185	2.31003	1.21000	0.00000	0.00000
0.33070	1.21000	0.00027	0.01551	2.35502	1.21000	-0.00000	-0.00000
0.37569	1.21000	-0.00007	-0.00416	2.40000	1.21000	0.00000	0.00000

TABLE IX. - SHROUD COORDINATES FOR CYLINDRICAL SHROUD EJECTOR NOZZLE

WITH SHROUD DIAMETER RATIO OF 1.11

Ratio of axial distance to radius of primary nozzle	Ratio of radial distance to radius of primary nozzle	Surface tangent	Surface angle, deg	Ratio of axial distance to radius of primary nozzle	Ratio of radial distance to radius of primary nozzle	Surface tangent	Surface angle, deg
-1.70364	1.36243	-0.14055	-8.00038	0.39146	1.11000	-0.00001	-0.00042
-1.65708	1.35589	-0.14054	-8.00014	0.43802	1.11000	0.00000	0.00011
-1.61052	1.34935	-0.14053	-7.99962	0.48458	1.11000	-0.00000	-0.00003
-1.56396	1.34280	-0.14054	-7.99969	0.53113	1.11000	0.00000	0.00001
-1.51741	1.33626	-0.14055	-8.00030	0.57769	1.11000	-0.00000	-0.00000
-1.47085	1.32972	-0.14055	-8.00033	0.62425	1.11000	0.00000	0.00000
-1.42429	1.32317	-0.14054	-8.00005	0.67081	1.11000	-0.00000	-0.00000
-1.37773	1.31663	-0.14053	-7.99956	0.71736	1.11000	0.00000	0.00000
-1.33117	1.31009	-0.14054	-7.99977	0.76392	1.11000	-0.00000	-0.00000
-1.28462	1.30354	-0.14055	-8.00028	0.81048	1.11000	0.00000	0.00000
-1.23806	1.29700	-0.14055	-8.00038	0.85704	1.11000	-0.00000	-0.00000
-1.19150	1.29046	-0.14054	-8.00003	0.90360	1.11000	0.00000	0.00000
-1.14494	1.28391	-0.14053	-7.99939	0.95015	1.11000	-0.00000	-0.00000
-1.09839	1.27737	-0.14054	-7.99992	0.99671	1.11000	0.00000	0.00000
-1.05183	1.27083	-0.14055	-8.00039	1.04327	1.11000	-0.00000	-0.00000
-1.00527	1.26428	-0.14055	-8.00027	1.08983	1.11000	0.00000	0.00000
-0.95871	1.25774	-0.14054	-7.99984	1.13638	1.11000	-0.00000	-0.00000
-0.91215	1.25120	-0.14053	-7.99953	1.18294	1.11000	0.00000	0.00000
-0.86560	1.24465	-0.14054	-8.00013	1.22950	1.11000	-0.00000	-0.00000
-0.81904	1.23811	-0.14055	-8.00035	1.27606	1.11000	0.00000	0.00000
-0.77248	1.23157	-0.14054	-8.00018	1.32261	1.11000	-0.00000	-0.00000
-0.72592	1.22502	-0.14054	-7.99974	1.36917	1.11000	0.00000	0.00000
-0.67937	1.21848	-0.14053	-7.99961	1.41573	1.11000	-0.00000	-0.00000
-0.63281	1.21194	-0.14054	-8.00015	1.46229	1.11000	0.00000	0.00000
-0.58625	1.20539	-0.14055	-8.00033	1.50885	1.11000	-0.00000	-0.00000
-0.53969	1.19885	-0.14054	-8.00020	1.55540	1.11000	0.00000	0.00000
-0.49314	1.19231	-0.14053	-7.99951	1.60196	1.11000	-0.00000	-0.00000
-0.44658	1.18577	-0.14053	-7.99967	1.64852	1.11000	0.00000	0.00000
-0.40002	1.17922	-0.14055	-8.00038	1.69508	1.11000	-0.00000	-0.00000
-0.35346	1.17268	-0.14055	-8.00031	1.74163	1.11000	0.00000	0.00000
-0.30690	1.16614	-0.14054	-7.99997	1.78819	1.11000	-0.00000	-0.00000
-0.26035	1.15959	-0.14053	-7.99962	1.83475	1.11000	0.00000	0.00000
-0.21379	1.15305	-0.14053	-7.99954	1.88131	1.11000	-0.00000	-0.00000
-0.16723	1.14651	-0.14057	-8.00183	1.92787	1.11000	0.00000	0.00000
-0.12067	1.13996	-0.14045	-7.99490	1.97442	1.11000	-0.00000	-0.00000
-0.07412	1.13342	-0.14090	-8.02000	2.02098	1.11000	0.00000	0.00000
-0.02756	1.12688	-0.13920	-7.92446	2.06754	1.11000	-0.00000	-0.00000
0.01900	1.12033	-0.14552	-8.27978	2.11410	1.11000	0.00000	0.00000
0.06556	1.11379	-0.12195	-6.95278	2.16065	1.11000	-0.00000	-0.00000
0.11211	1.11000	-0.03217	-1.84266	2.20721	1.11000	0.00000	0.00000
0.15867	1.11004	0.00918	0.52584	2.25377	1.11000	-0.00000	-0.00000
0.20523	1.11003	-0.00300	-0.17199	2.30033	1.11000	0.00000	0.00000
0.25179	1.11000	0.00038	0.02162	2.34688	1.11000	-0.00000	-0.00000
0.29835	1.11000	-0.00010	-0.00579	2.39344	1.11000	0.00000	0.00000
0.34490	1.11000	0.00003	0.00155	2.44000	1.11000	-0.00000	-0.00000

TABLE X. - SHROUD COORDINATES FOR CYLINDRICAL SHROUD EJECTOR NOZZLE

WITH SHROUD DIAMETER RATIO OF 1.21

Ratio of axial distance to radius of primary nozzle	Ratio of radial distance to radius of primary nozzle	Surface tangent	Surface angle, deg	Ratio of axial distance to radius of primary nozzle	Ratio of radial distance to radius of primary nozzle	Surface tangent	Surface angle, deg
-1.75364	1.31243	-0.14055	-8.00049	0.12405	1.06003	-0.00188	-0.10784
-1.71191	1.30657	-0.14055	-8.00030	0.16577	1.06000	-0.00005	-0.00291
-1.67018	1.30070	-0.14054	-7.99973	0.20750	1.06000	0.00001	0.00078
-1.62846	1.29484	-0.14053	-7.99941	0.24922	1.06000	-0.00000	-0.00021
-1.58673	1.28898	-0.14054	-8.00004	0.29095	1.06000	0.00000	0.00006
-1.54500	1.28311	-0.14055	-8.00037	0.33268	1.06000	-0.00000	-0.00002
-1.50328	1.27725	-0.14055	-8.00027	0.37440	1.06000	0.00000	0.00000
-1.46155	1.27138	-0.14054	-7.99997	0.41613	1.06000	-0.00000	-0.00000
-1.41983	1.26552	-0.14053	-7.99947	0.45786	1.06000	0.00000	0.00000
-1.37810	1.25966	-0.14054	-7.99981	0.49958	1.06000	-0.00000	-0.00000
-1.33637	1.25379	-0.14055	-8.00028	0.54131	1.06000	0.00000	0.00000
-1.29465	1.24793	-0.14055	-8.00033	0.58303	1.06000	-0.00000	-0.00000
-1.25292	1.24206	-0.14054	-8.00018	0.62476	1.06000	0.00000	0.00000
-1.21119	1.23620	-0.14053	-7.99953	0.66649	1.06000	-0.00000	-0.00000
-1.16947	1.23033	-0.14053	-7.99959	0.70821	1.06000	0.00000	0.00000
-1.12774	1.22447	-0.14055	-8.00029	0.74994	1.06000	-0.00000	-0.00000
-1.08602	1.21861	-0.14055	-8.00032	0.79167	1.06000	0.00000	0.00000
-1.04429	1.21274	-0.14054	-8.00018	0.83339	1.06000	-0.00000	-0.00000
-1.00256	1.20688	-0.14054	-7.99982	0.87512	1.06000	0.00000	0.00000
-0.96084	1.20101	-0.14053	-7.99953	0.91684	1.06000	-0.00000	-0.00000
-0.91911	1.19515	-0.14054	-8.00009	0.95857	1.06000	0.00000	0.00000
-0.87738	1.18928	-0.14055	-8.00036	1.00030	1.06000	-0.00000	-0.00000
-0.83566	1.18342	-0.14055	-8.00027	1.04202	1.06000	0.00000	0.00000
-0.79393	1.17756	-0.14054	-7.99996	1.08375	1.06000	-0.00000	-0.00000
-0.75221	1.17169	-0.14053	-7.99946	1.12547	1.06000	0.00000	0.00000
-0.71048	1.16583	-0.14054	-7.99984	1.16720	1.06000	-0.00000	-0.00000
-0.66875	1.15996	-0.14055	-8.00027	1.20893	1.06000	0.00000	0.00000
-0.62703	1.15410	-0.14055	-8.00032	1.25065	1.06000	-0.00000	-0.00000
-0.58530	1.14823	-0.14054	-8.00020	1.29238	1.06000	0.00000	0.00000
-0.54357	1.14237	-0.14053	-7.99950	1.33411	1.06000	-0.00000	-0.00000
-0.50185	1.13651	-0.14053	-7.99958	1.37583	1.06000	0.00000	0.00000
-0.46012	1.13064	-0.14055	-8.00032	1.41756	1.06000	-0.00000	-0.00000
-0.41840	1.12478	-0.14055	-8.00033	1.45928	1.06000	0.00000	0.00000
-0.37667	1.11891	-0.14054	-8.00016	1.50101	1.06000	-0.00000	-0.00000
-0.33494	1.11305	-0.14054	-7.99980	1.54274	1.06000	0.00000	0.00000
-0.29322	1.10718	-0.14053	-7.99948	1.58446	1.06000	-0.00000	-0.00000
-0.25149	1.10132	-0.14055	-8.00028	1.62619	1.06000	0.00000	0.00000
-0.20976	1.09546	-0.14054	-7.99970	1.66792	1.06000	-0.00000	-0.00000
-0.16804	1.08959	-0.14059	-8.00272	1.70964	1.06000	0.00000	0.00000
-0.12631	1.08373	-0.14038	-7.99079	1.75137	1.06000	-0.00000	-0.00000
-0.08459	1.07786	-0.14114	-8.03368	1.79309	1.06000	0.00000	0.00000
-0.04286	1.07200	-0.13826	-7.87209	1.83482	1.06000	-0.00000	-0.00000
-0.00113	1.06614	-0.14903	-8.47631	1.87655	1.06000	0.00000	0.00000
0.04059	1.06076	-0.07405	-4.23496	1.91827	1.06000	-0.00000	-0.00000
0.08232	1.06003	0.00600	0.34367	1.96000	1.06000	0.00000	0.00000

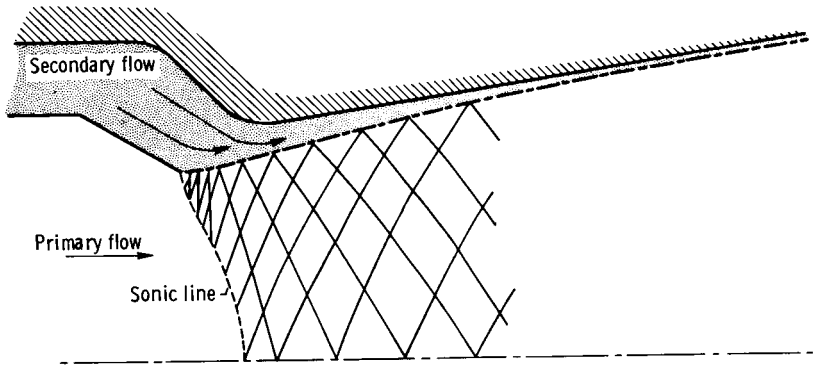

Figure 1. - Supersonic ejector system.

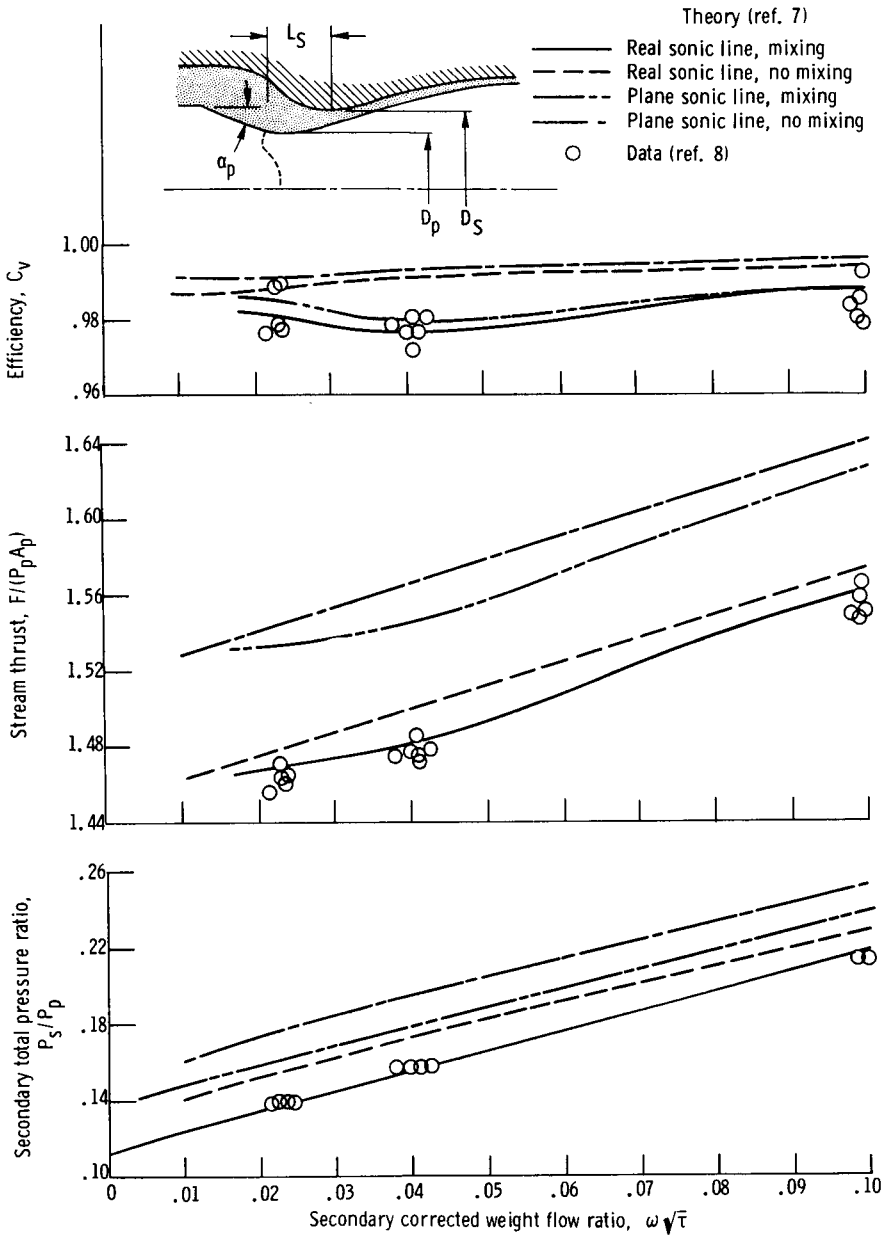

Figure 2. - Influence of sonic line and mixing process on performance of a convergent-divergent contoured flap ejector. Shroud shoulder diameter ratio, D_S/D_0, 1.37; spacing ratio, L_S/D_p, 0.5; primary nozzle lip angle, α_p, 27°; Reynolds number, Re, 3.3×10^6; ratio of primary total pressure to free-stream static pressure, P_p/p_0, 27.

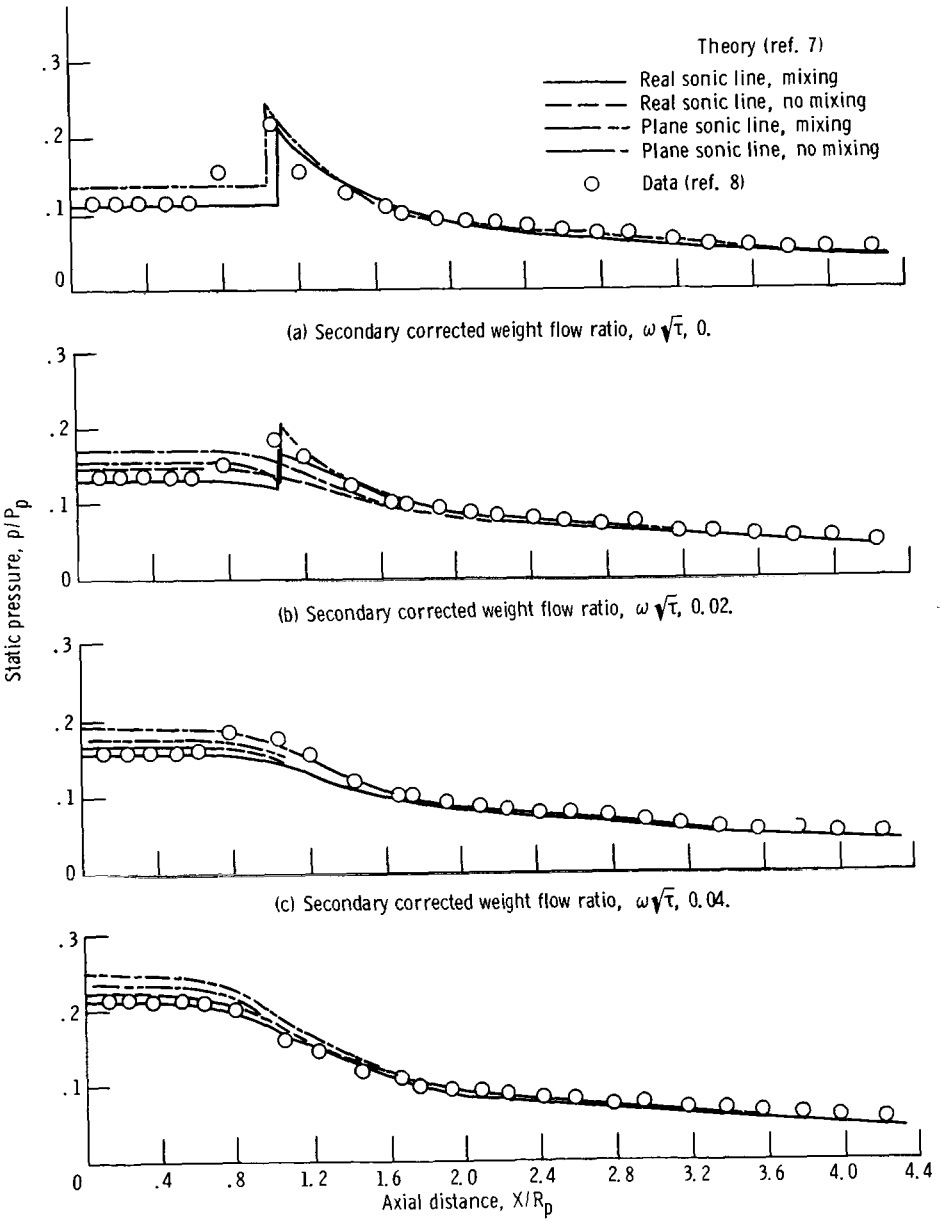

(a) Secondary corrected weight flow ratio, $\omega\sqrt{\tau}$, 0.

(b) Secondary corrected weight flow ratio, $\omega\sqrt{\tau}$, 0.02.

(c) Secondary corrected weight flow ratio, $\omega\sqrt{\tau}$, 0.04.

(d) Secondary corrected weight flow ratio, $\omega\sqrt{\tau}$, 0.10.

Figure 3. - Influence of sonic line and mixing process on shroud static pressure distribution of a convergent-divergent ejector nozzle. Shroud shoulder diameter ratio, D_S/D_p, 1.37; spacing ratio, L_S/D_p, 0.5; primary nozzle lip angle, α_p, 27^0.

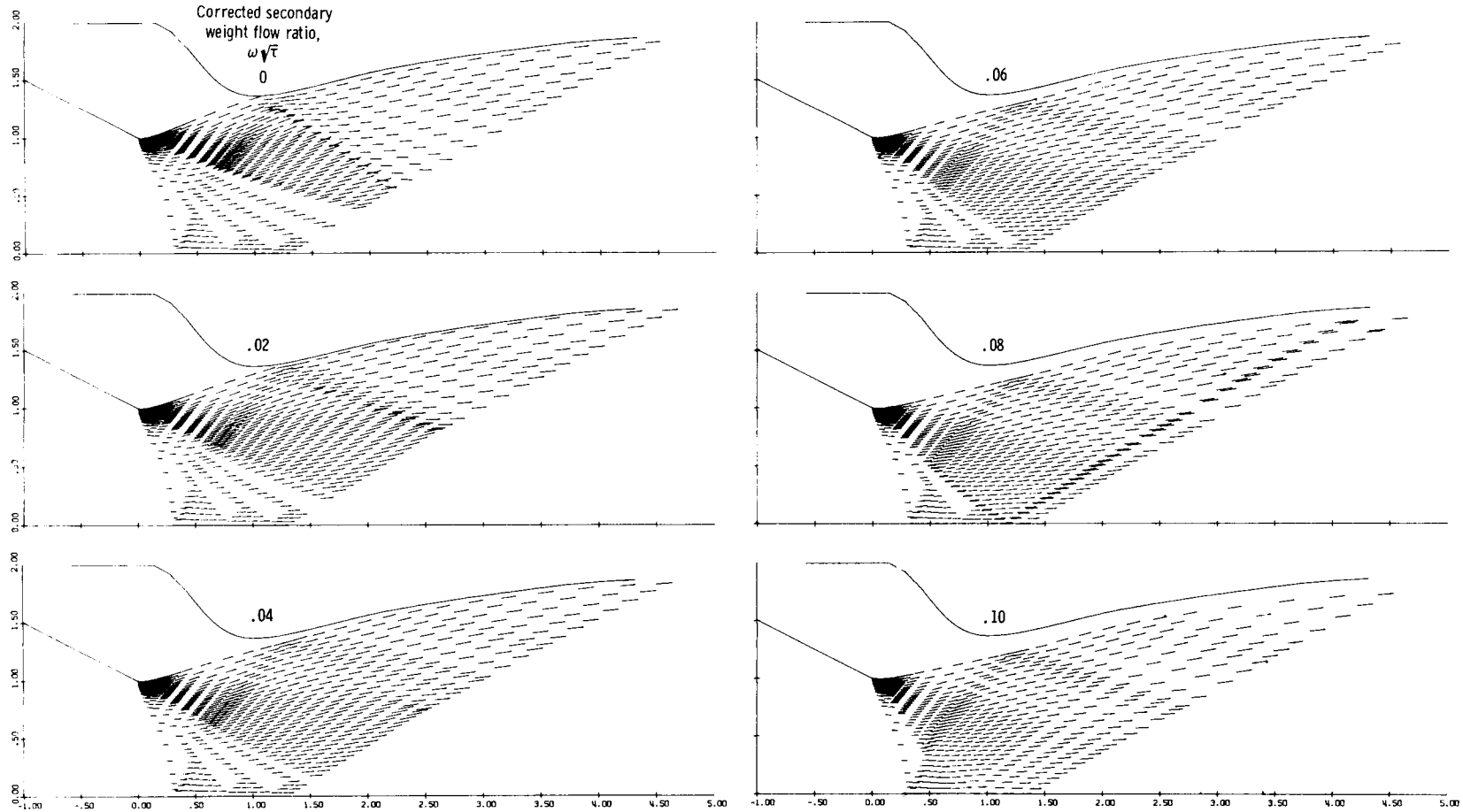

Figure 4. - Influence of secondary flow on the flow field of a convergent-divergent contoured flap ejector. Shroud shoulder diameter ratio, D_S/D_p, 1.37; spacing ratio, L_S/D_p, 0.5.

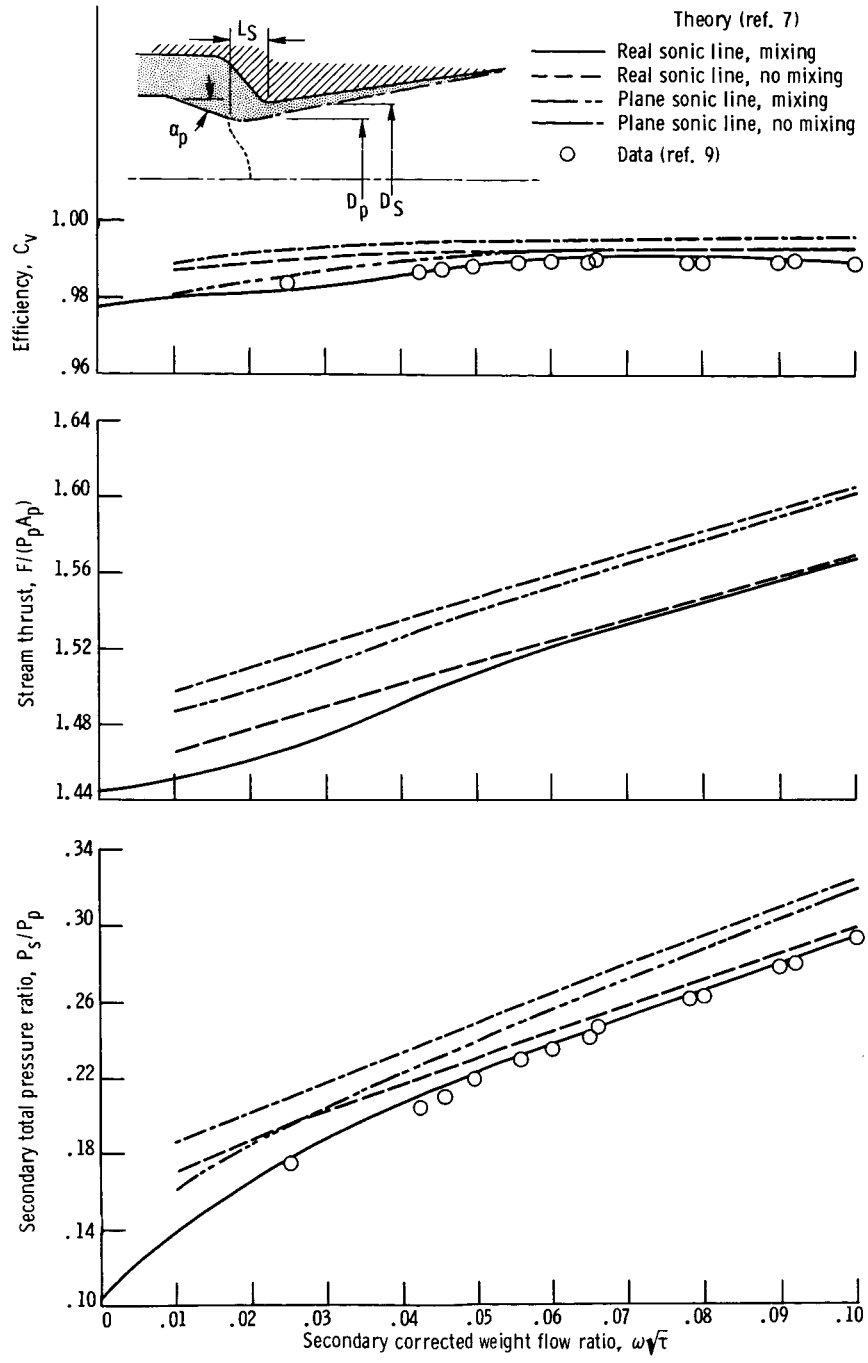

Figure 5. - Influence of sonic line and mixing process on performance of a convergent-divergent conical flap ejector. Shroud shoulder diameter ratio, D_S/D_p, 1.225; spacing ratio, L_S/D_p, 0.22; primary nozzle lip angle, α_p, 16^0; Reynolds number, Re, 4.4×10^6; ratio of primary total pressure to free-stream static pressure, P_p/p_0, 14.

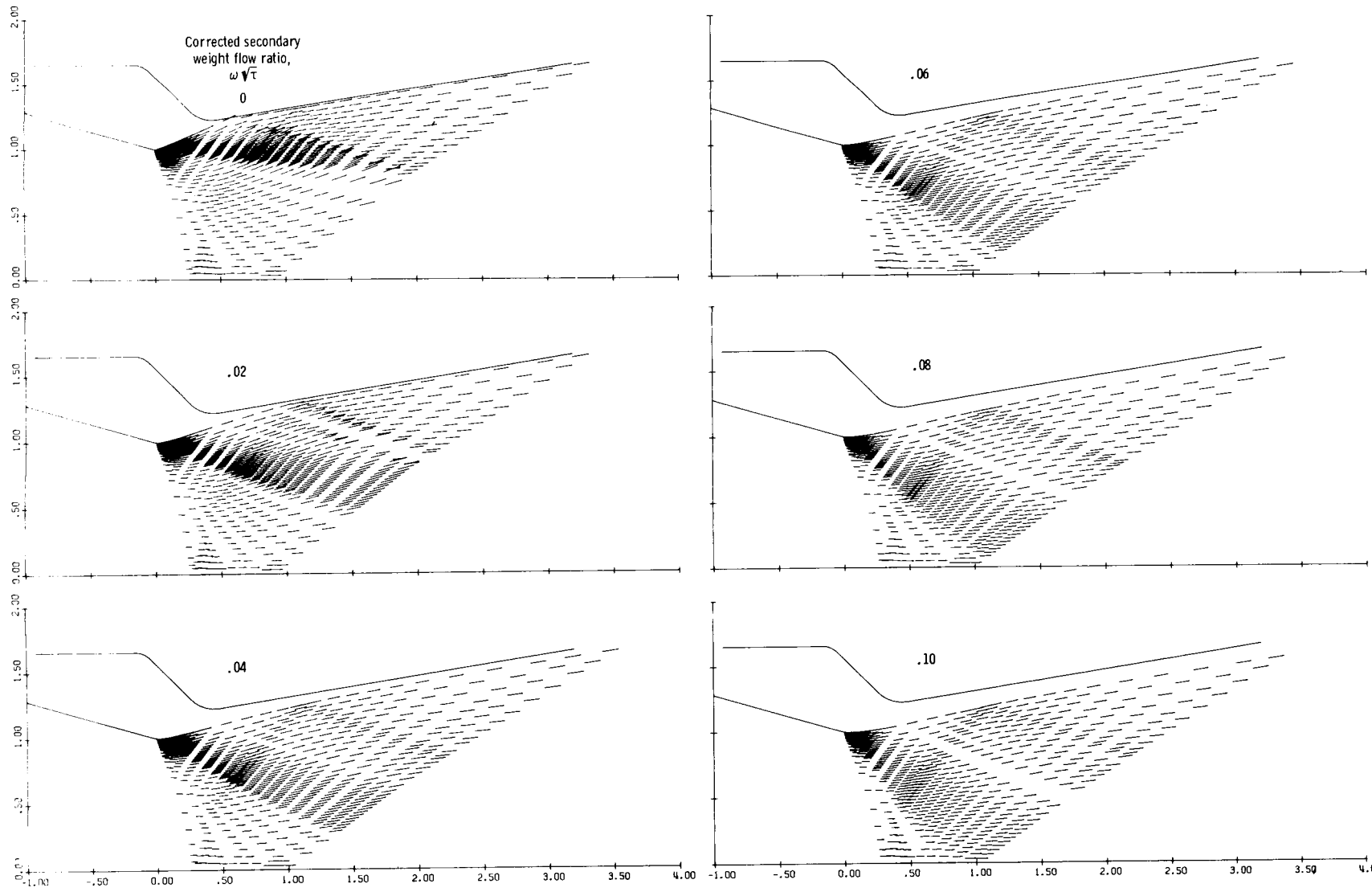

Figure 6. - Influence of secondary flow on the flow field of a convergent-divergent conical flap ejector. Shroud shoulder diameter ratio, D_S/D_p, 1.225; spacing ratio, L_S/D_p, 0.22.

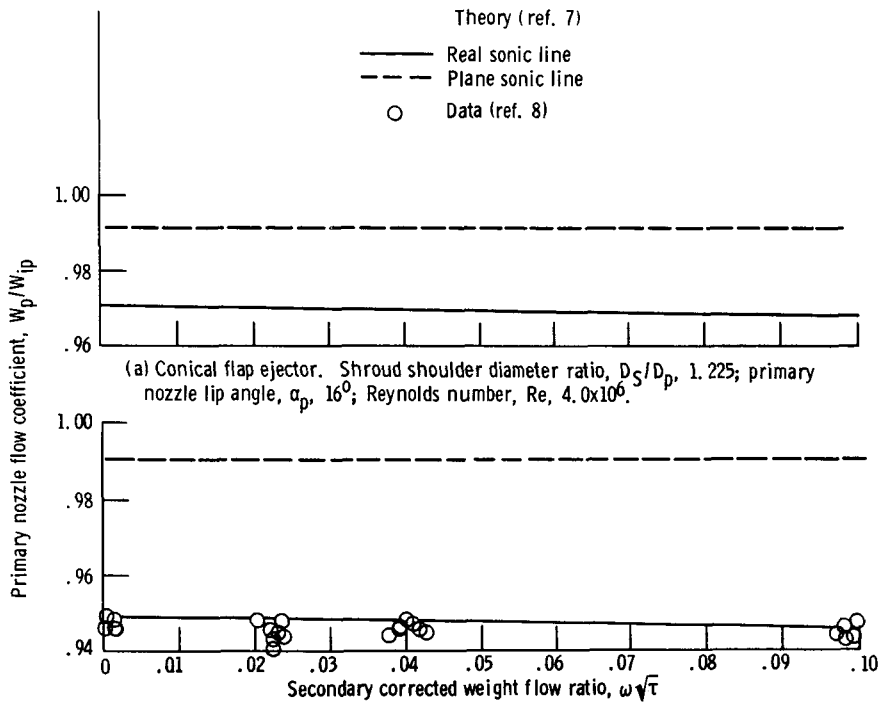

(a) Conical flap ejector. Shroud shoulder diameter ratio, D_S/D_p, 1.225; primary nozzle lip angle, α_p, 16^0; Reynolds number, Re, 4.0×10^6.

(b) Contoured shroud ejector. $D_S/D_p = 1.32$; $\alpha_p = 27^0$; $Re = 3.3 \times 10^6$.

Figure 7. - Influence of sonic line on primary nozzle mass flow.

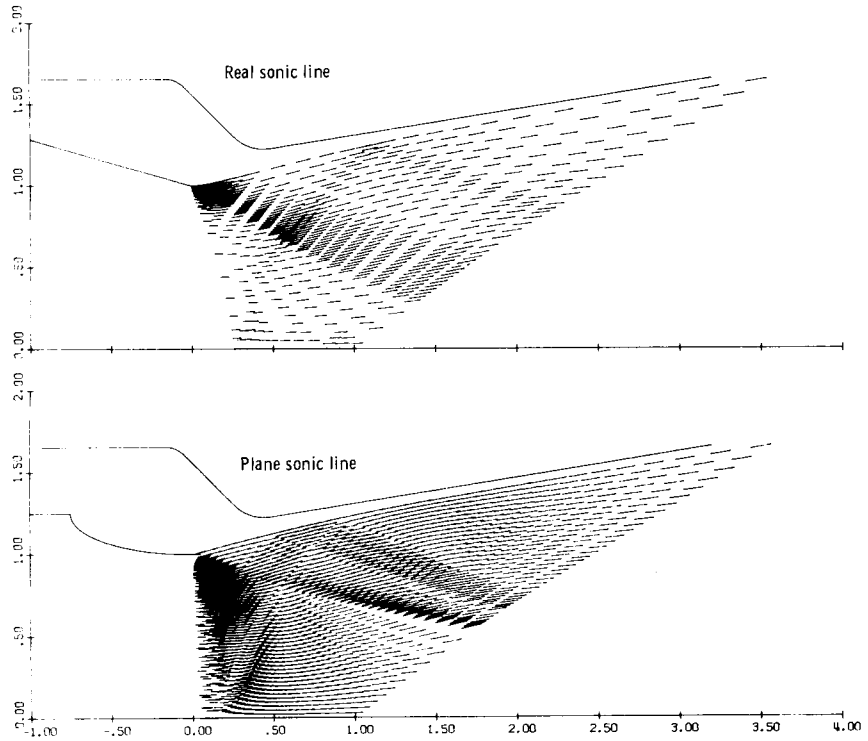

(a) Conical flap ejector. Shroud shoulder diameter ratio, D_S/D_p, 1.225; spacing ratio, L_S/D_p, 0.22.

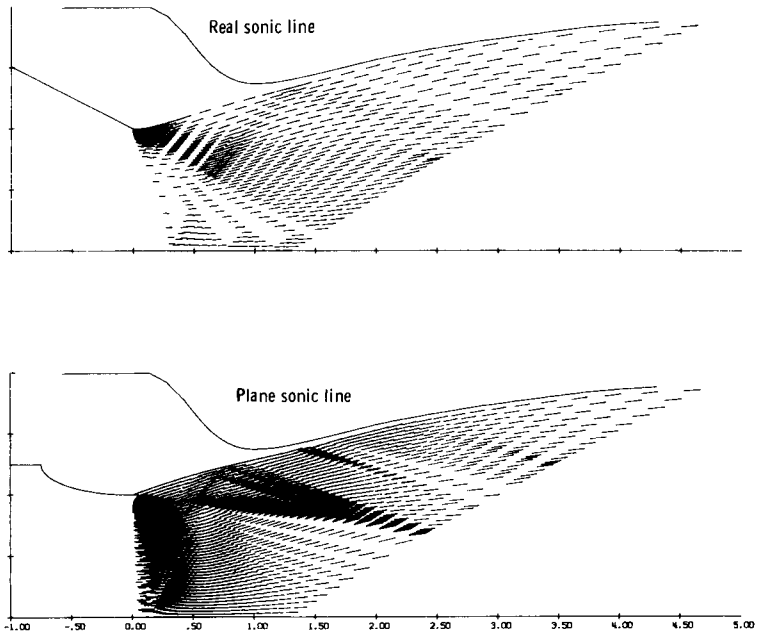

(b) Contoured flap ejector. D_S/D_p = 1.37; L_S/D_p = 0.5.

Figure 8. - Influence of sonic line on the flow field of a convergent-divergent ejector nozzle. Secondary weight flow ratio, $\omega\sqrt{\tau}$, 0.04.

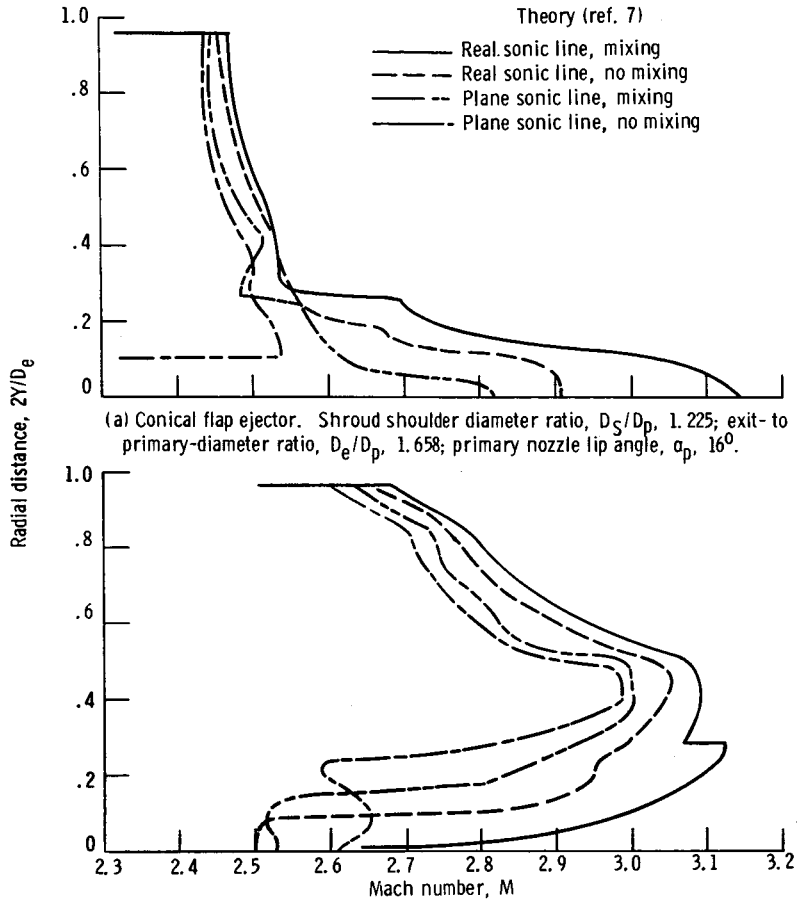

(a) Conical flap ejector. Shroud shoulder diameter ratio, D_S/D_p, 1.225; exit-to primary-diameter ratio, D_e/D_p, 1.658; primary nozzle lip angle, α_p, 16^0.

(b) Contoured flap ejector. $D_S/D_p = 1.37$; $D_e/D_p = 1.87$; $\alpha_p = 27^0$.

Figure 9. - Influence of conic line and mixing process on ejector exit Mach number profiles. Corrected secondary weight flow ratio, $\omega\sqrt{\tau}$, 0.04.

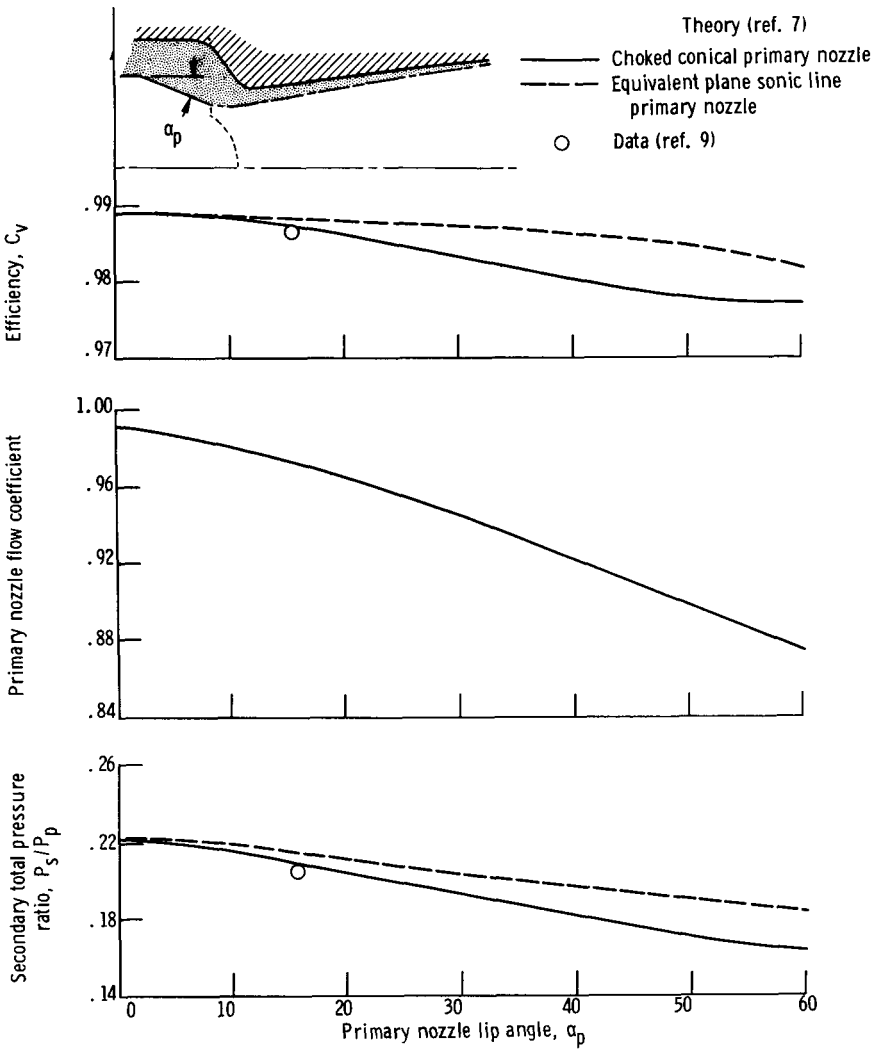

Figure 10. - Effect of primary nozzle lip angle on performance of a convergent-divergent conical flap ejector. Corrected secondary weight flow ratio, $\omega\sqrt{\tau}$, 0.04; ratio of primary total pressure to free-stream static pressure, P_p/p_0, 10; Reynolds number, Re, 4.0×10^6.

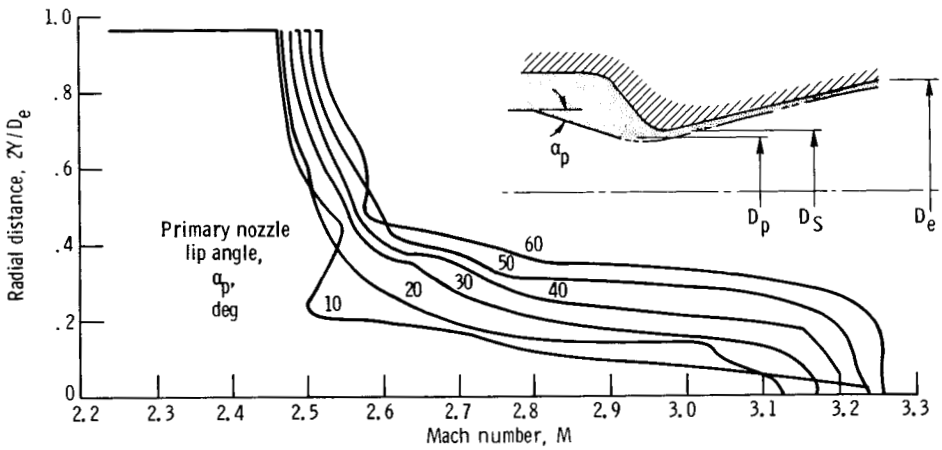

Figure 11. - Effect of primary nozzle lip angle on exit Mach number profile for a convergent-divergent conical flap ejector. Shroud shoulder diameter ratio, D_S/D_p, 1.225; exit- to primary-diameter ratio, D_e/D_p, 1.658; corrected secondary weight flow ratio, $\omega\sqrt{\tau}$, 0.04.

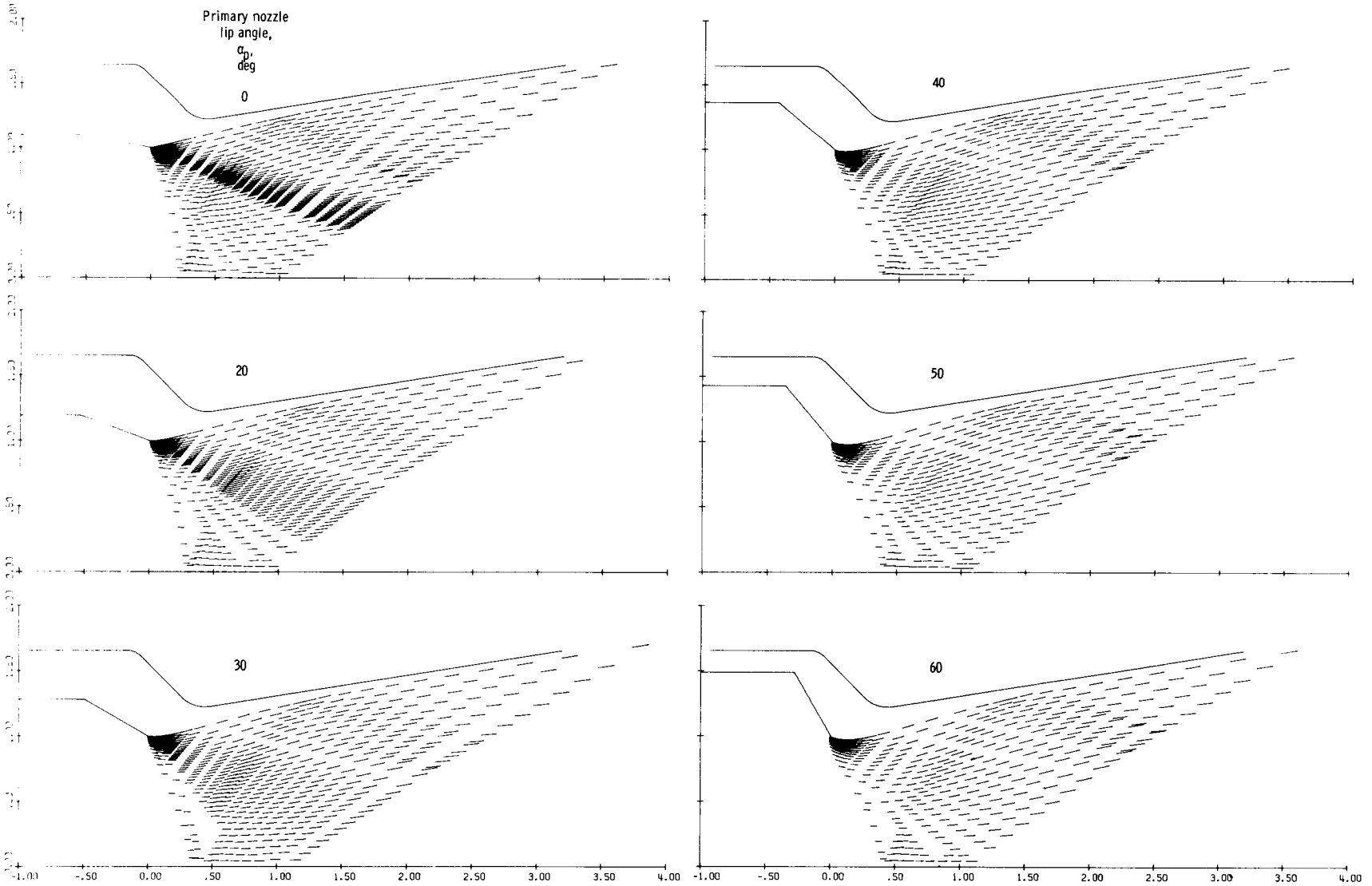

Figure 12. - Influence of primary nozzle lip angle on the flow field of a convergent-divergent conical flap ejector. Shroud shoulder diameter ratio, D_S/D_p, 1.225; spacing ratio, L_S/D_p, 0.22.

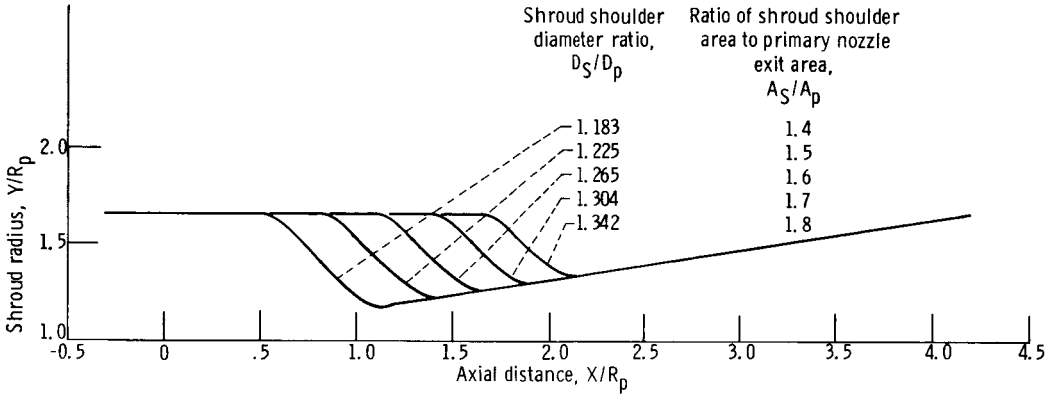

Figure 13. - Shroud geometry for a family of conical flap ejector nozzles. (Data from ref. 9.)

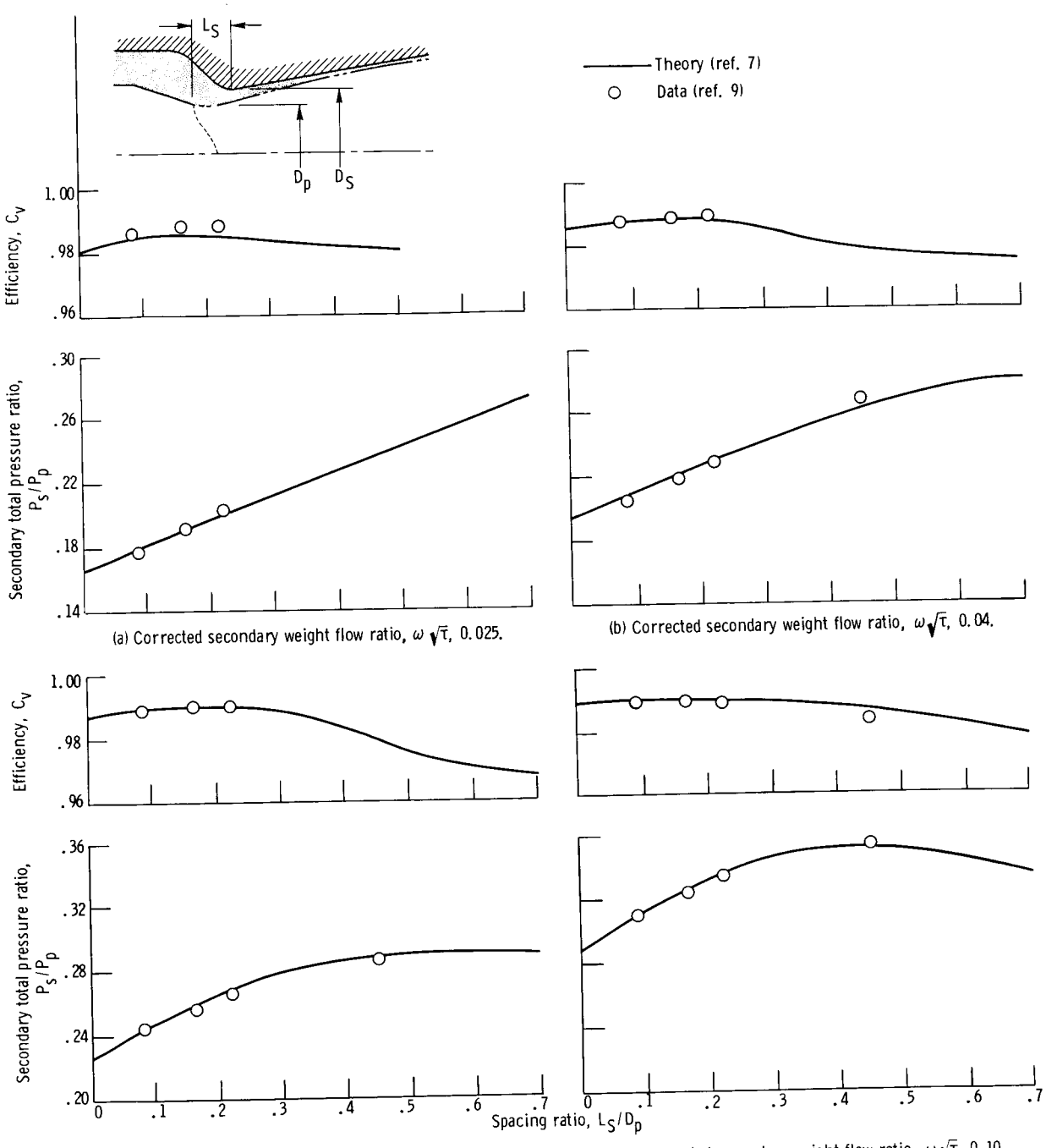

Figure 14. - Effect of spacing ratio on performance of a convergent-divergent conical flap ejector nozzle with a shroud shoulder diameter ratio D_S/D_p of 1.183 (A_S/A_p = 1.4), a Reynolds number Re of 4.0×10^6, and a ratio of primary total pressure to free-stream static pressure P_p/p_0 of 14.

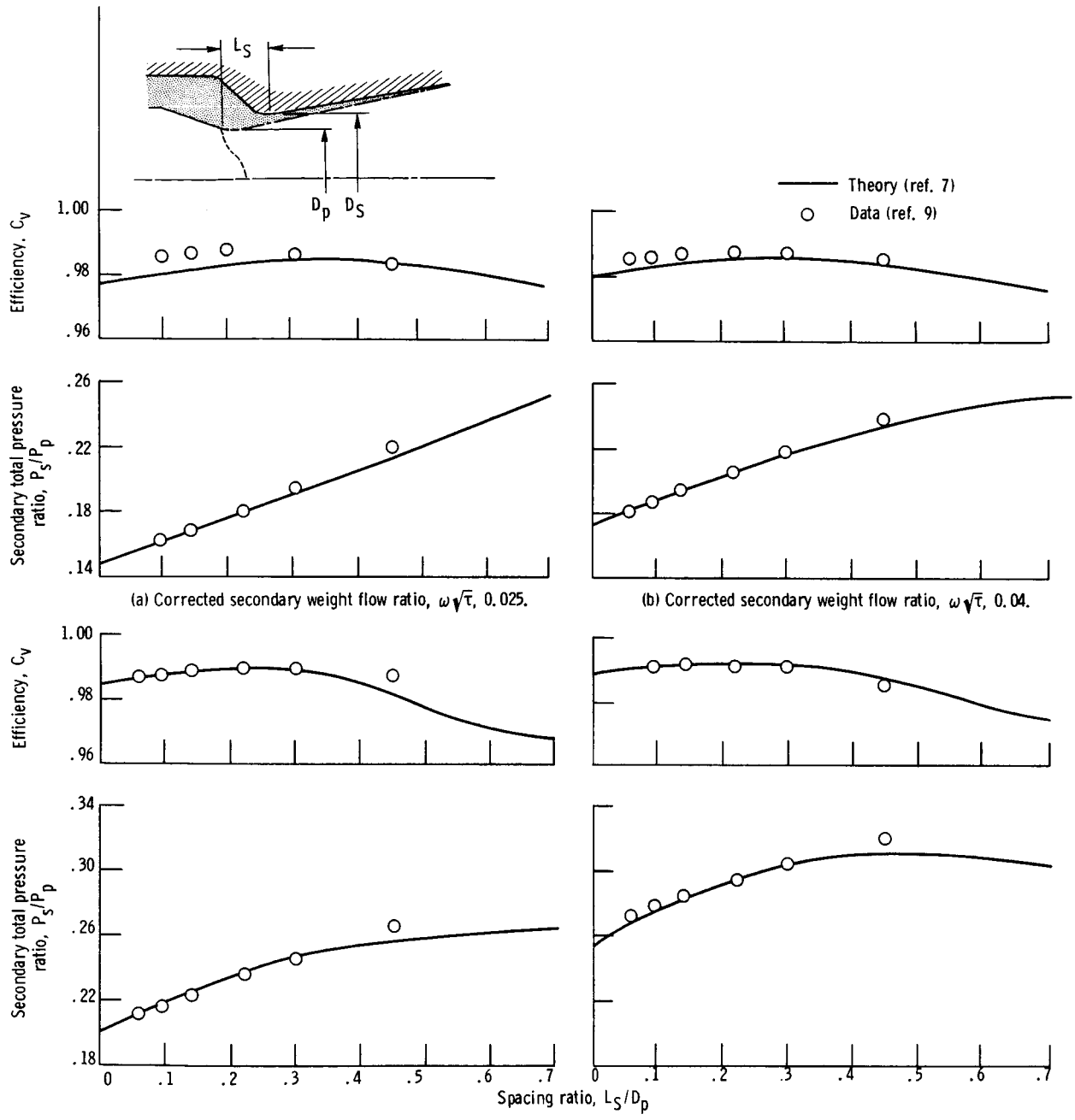

Figure 15. - Effect of spacing ratio on performance of a convergent-divergent conical flap ejector with a shroud shoulder diameter ratio D_S/D_p of 1.225 (A_S/A_p = 1.5), a Reynolds number Re of 4.0×10^6, and a ratio of primary total pressure to free-stream static pressure P_p/p_0 of 14.

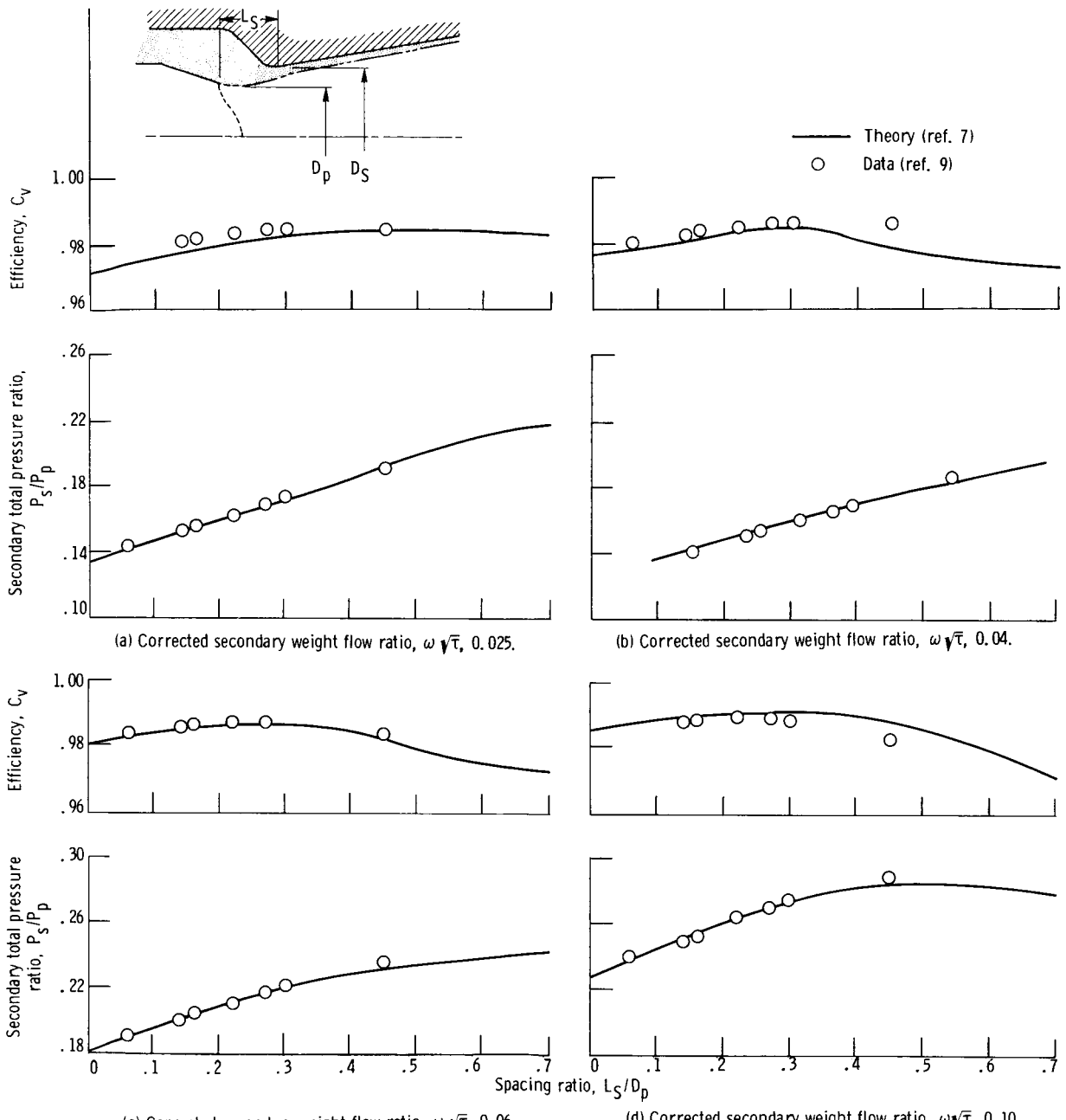

Figure 16. - Effect of spacing ratio on performance of a convergent-divergent conical flap ejector with a shroud shoulder diameter ratio D_S/D_p of 1.265 (A_S/A_p = 1.6), a Reynolds number Re of 4.0×10^6, and a ratio of primary total pressure to free-stream static pressure P_p/p_0 of 14.

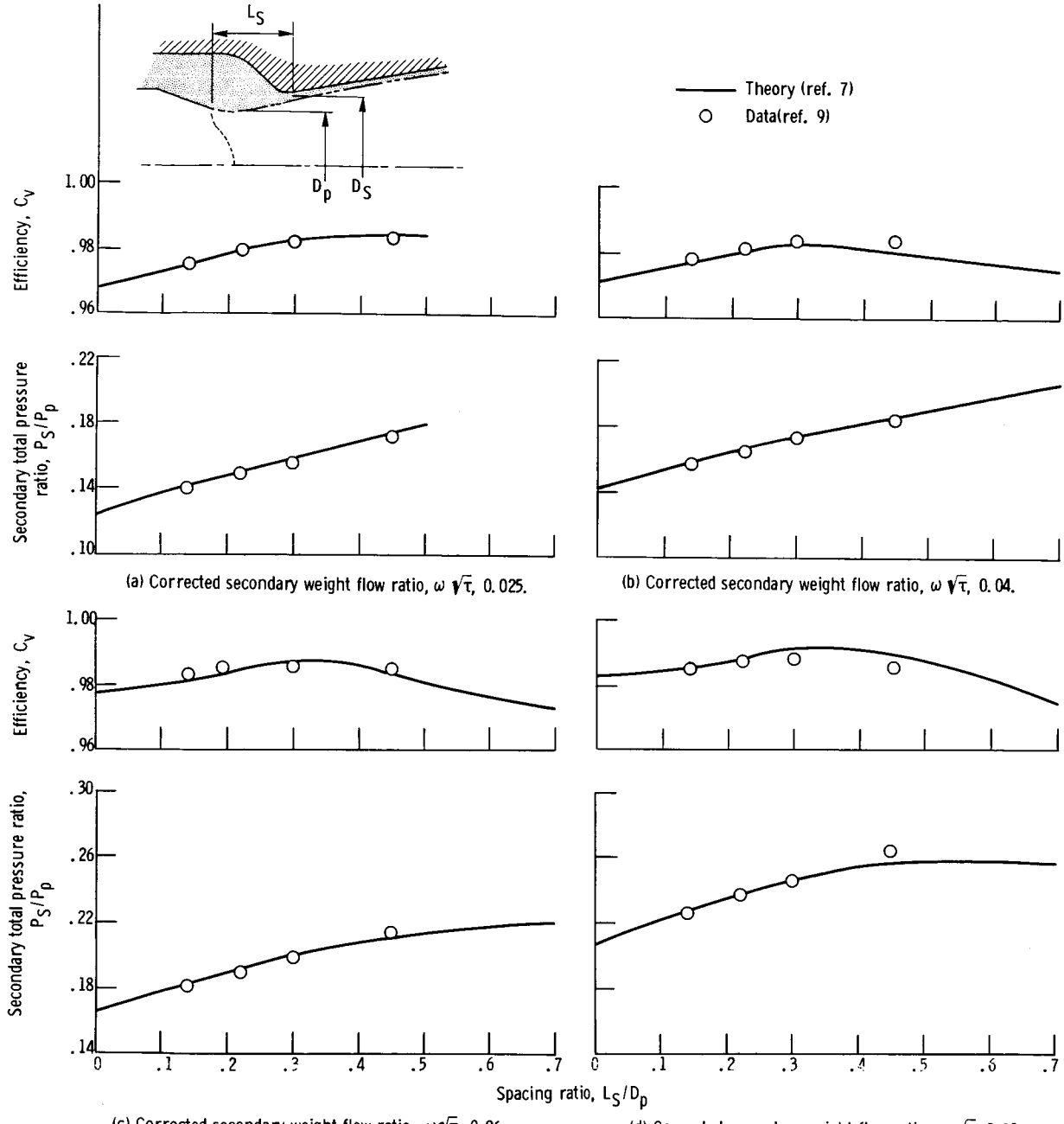

Figure 17. - Effect of spacing ratio on performance of a convergent-divergent conical flap ejector with a shroud shoulder diameter ratio D_S/D_p of 1.304 (A_S/A_p = 1.7), a Reynolds number Re of 4.0×10^6, and a ratio of primary total pressure to free-stream static pressure of P_s/p_0 of 14.

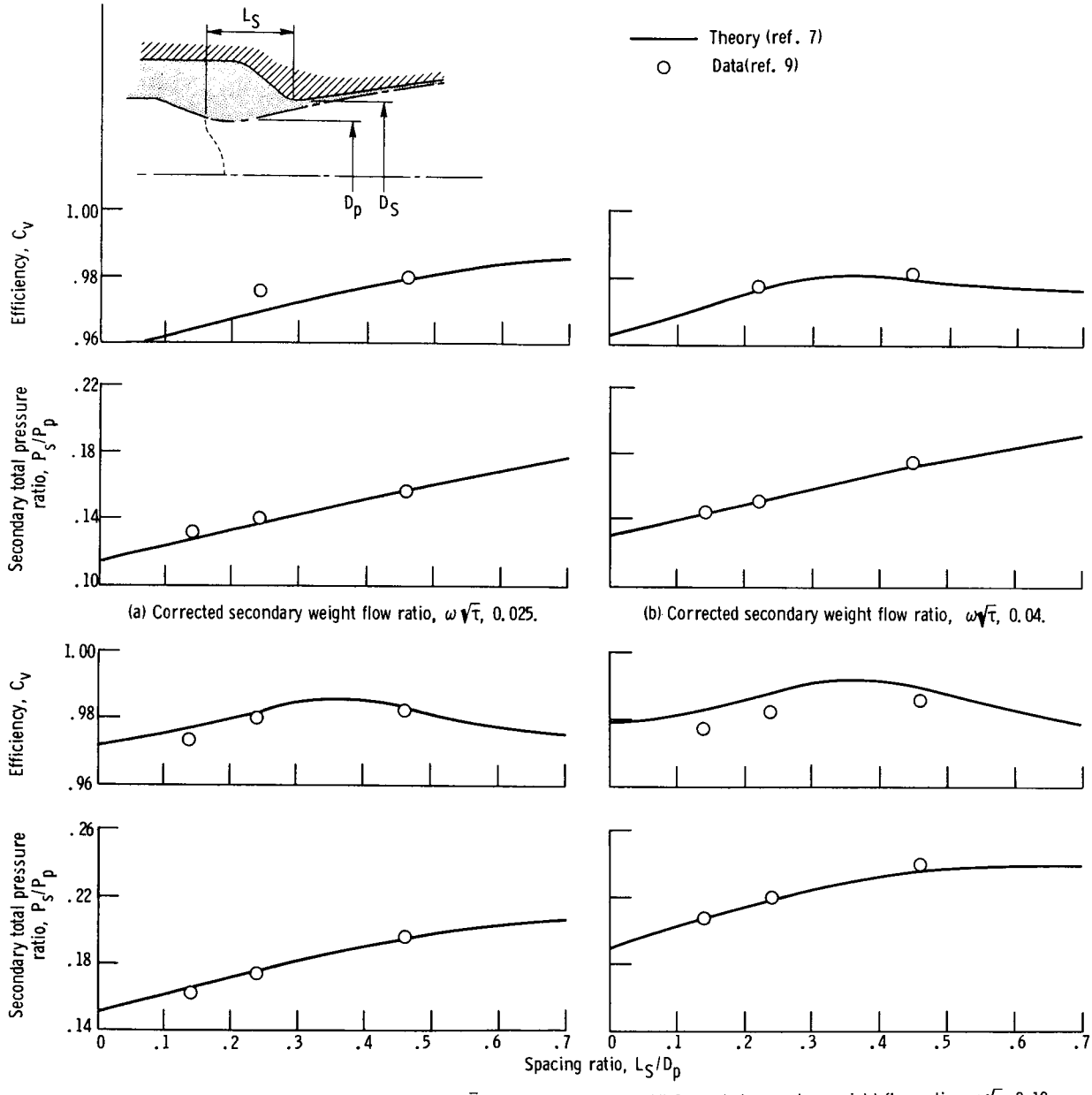

Figure 18. - Effect of spacing ratio on performance of a convergent-divergent conical flap ejector with a shroud shoulder diameter ratio D_S/D_p of 1.342 (A_S/A_p = 1.8), a Reynolds number Re of 4.0×10^6, and a ratio of primary total pressure to free-stream static pressure P_p/p_0 of 14.

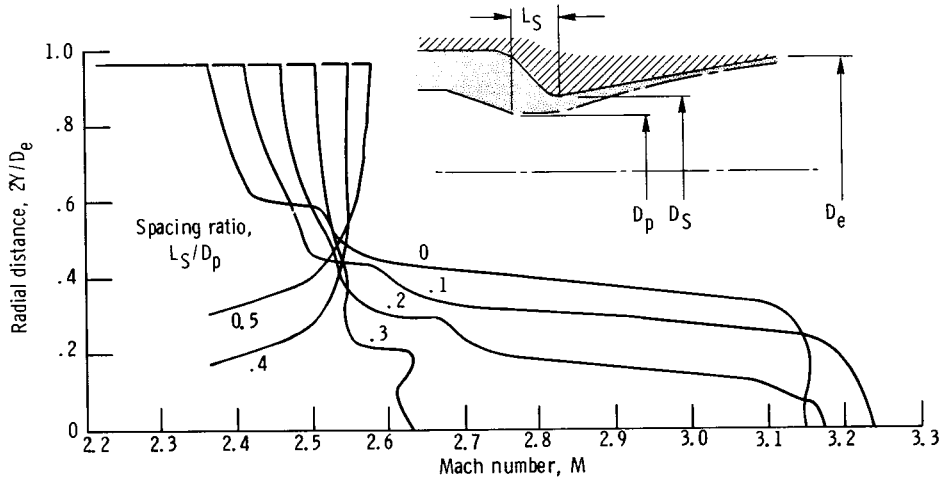

Figure 19. - Effect of spacing ratio on exit Mach number profile for a convergent-divergent conical flap ejector. Shroud shoulder diameter ratio, D_S/D_p, 1.225; ratio of exit diameter to primary diameter, D_e/D_p, 1.658; corrected secondary weight flow ratio, $\omega\sqrt{\tau}$, 0.04.

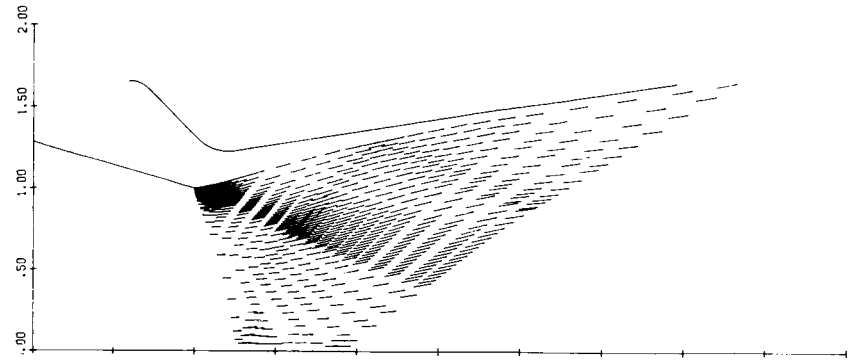

(a) Spacing ratio, L_S/D_p, 0.1.

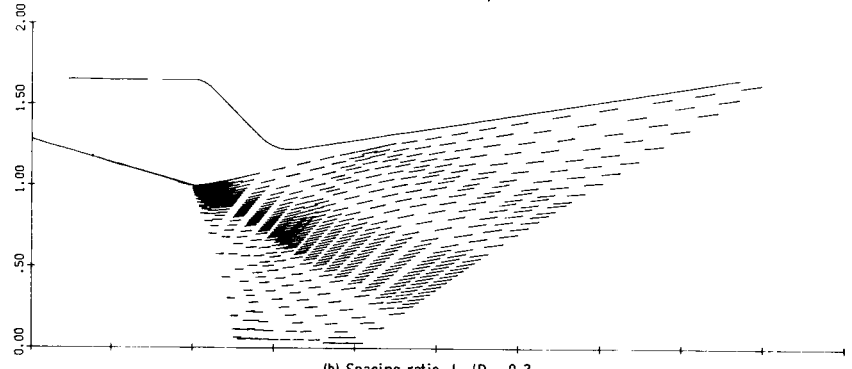

(b) Spacing ratio, L_S/D_p, 0.3.

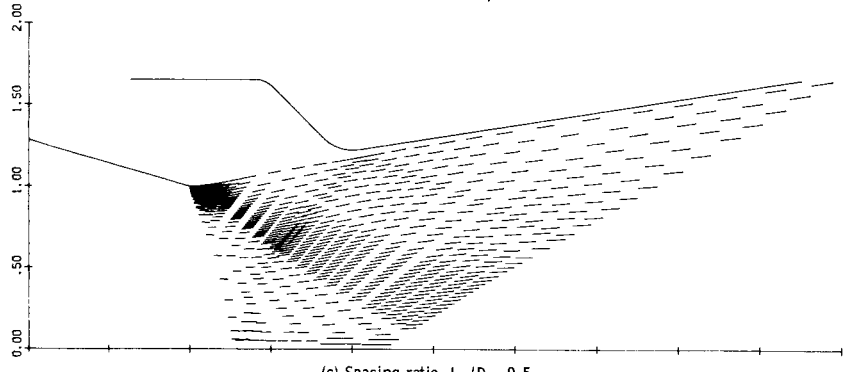

(c) Spacing ratio, L_S/D_p, 0.5.

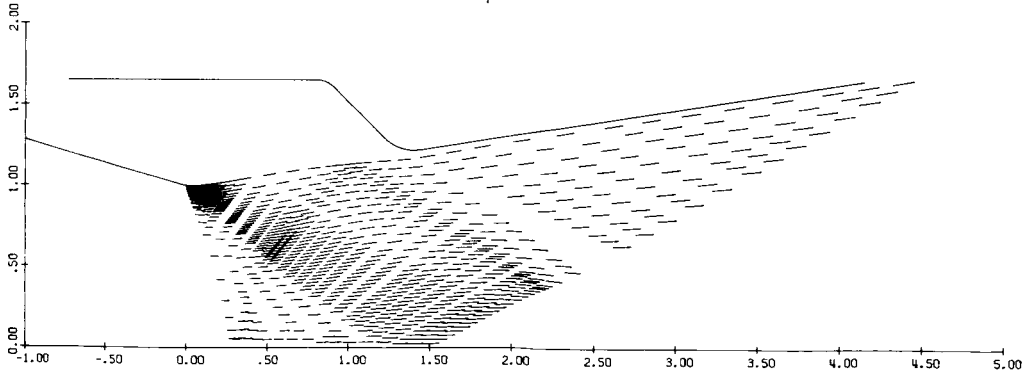

(d) Spacing ratio, L_S/D_p, 0.7.

Figure 20. - Influence of spacing ratio on the flow field of a convergent-divergent conical flap ejector. Corrected secondary weight flow ratio, $\omega\sqrt{\tau}$, 0.04; shroud shoulder diameter ratio, D_S/D_p, 1.225.

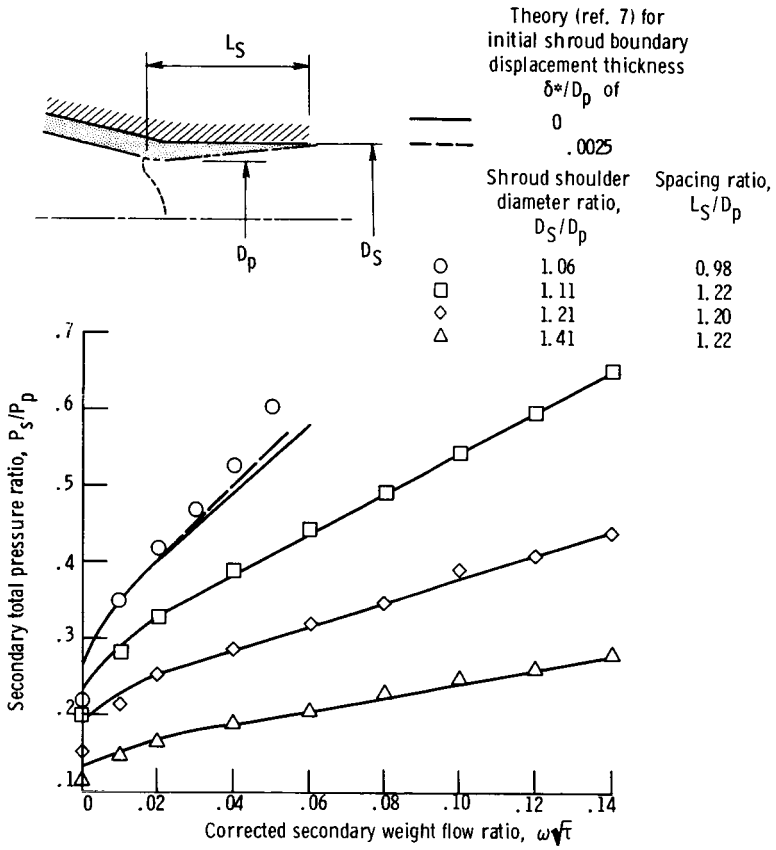

Figure 21. - Effect of shroud shoulder diameter ratio on pumping characteristics of a cylindrical shroud ejector. Primary nozzle lip angle, α_p, 8°; Reynolds number, Re, 3.5×10^6.

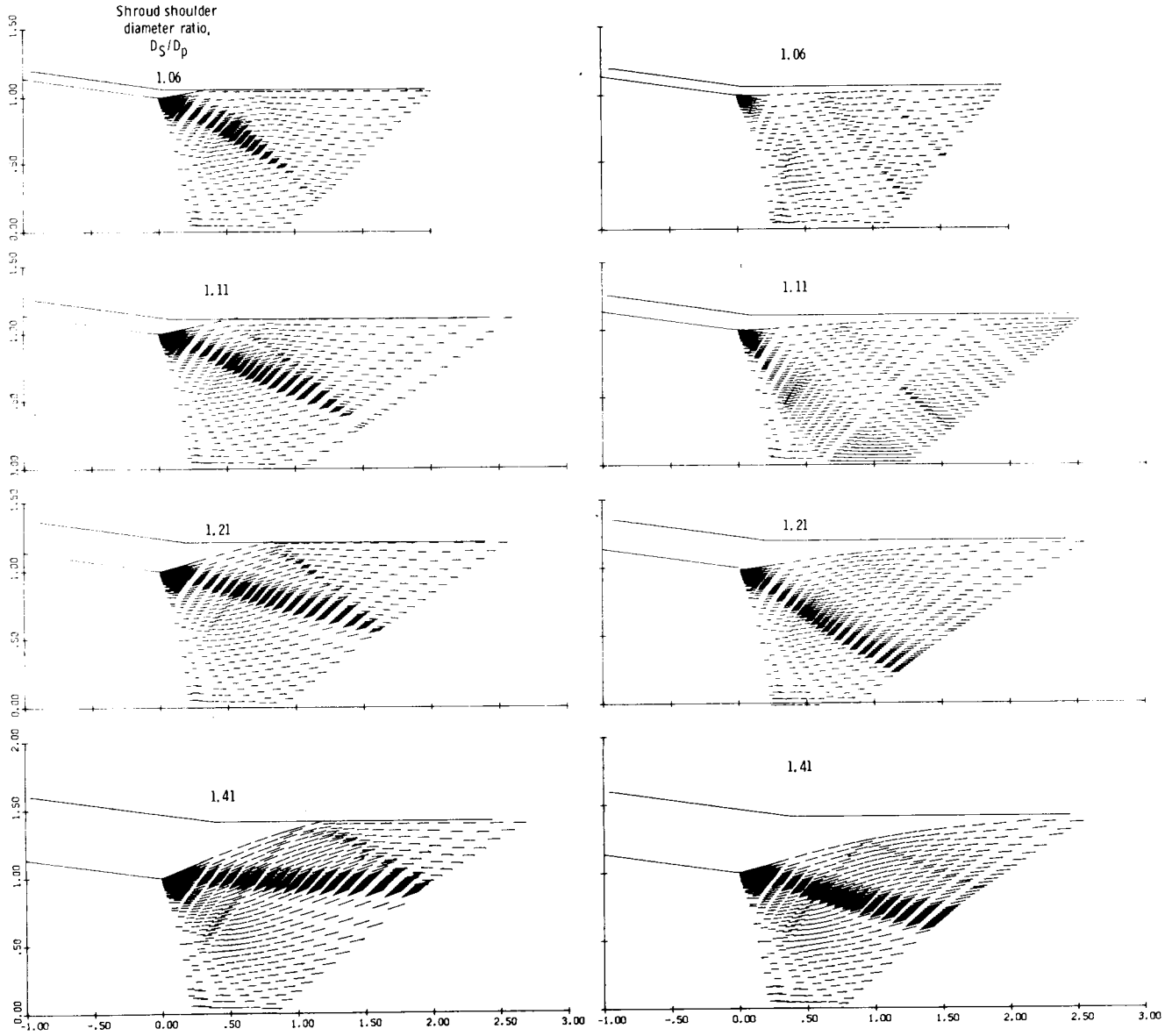

(a) Corrected secondary weight flow ratio, $\omega\sqrt{\tau}$, 0.

(b) Corrected secondary weight flow ratio, $\omega\sqrt{\tau}$, 0.04.

Figure 22. - Influence of shroud shoulder diameter ratio on the flow field of a cylindrical shroud ejector nozzle.

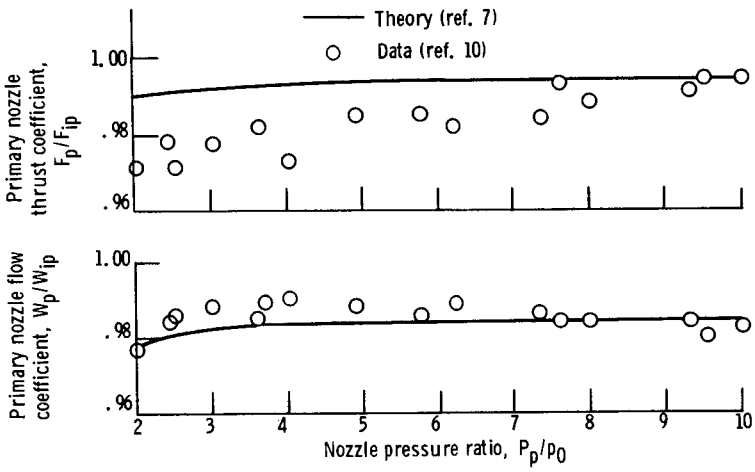

Figure 23. - Performance of a choked conical primary nozzle. Primary nozzle lip angle, α_p, 8^0; Reynolds number, Re, 3.5×10^6.

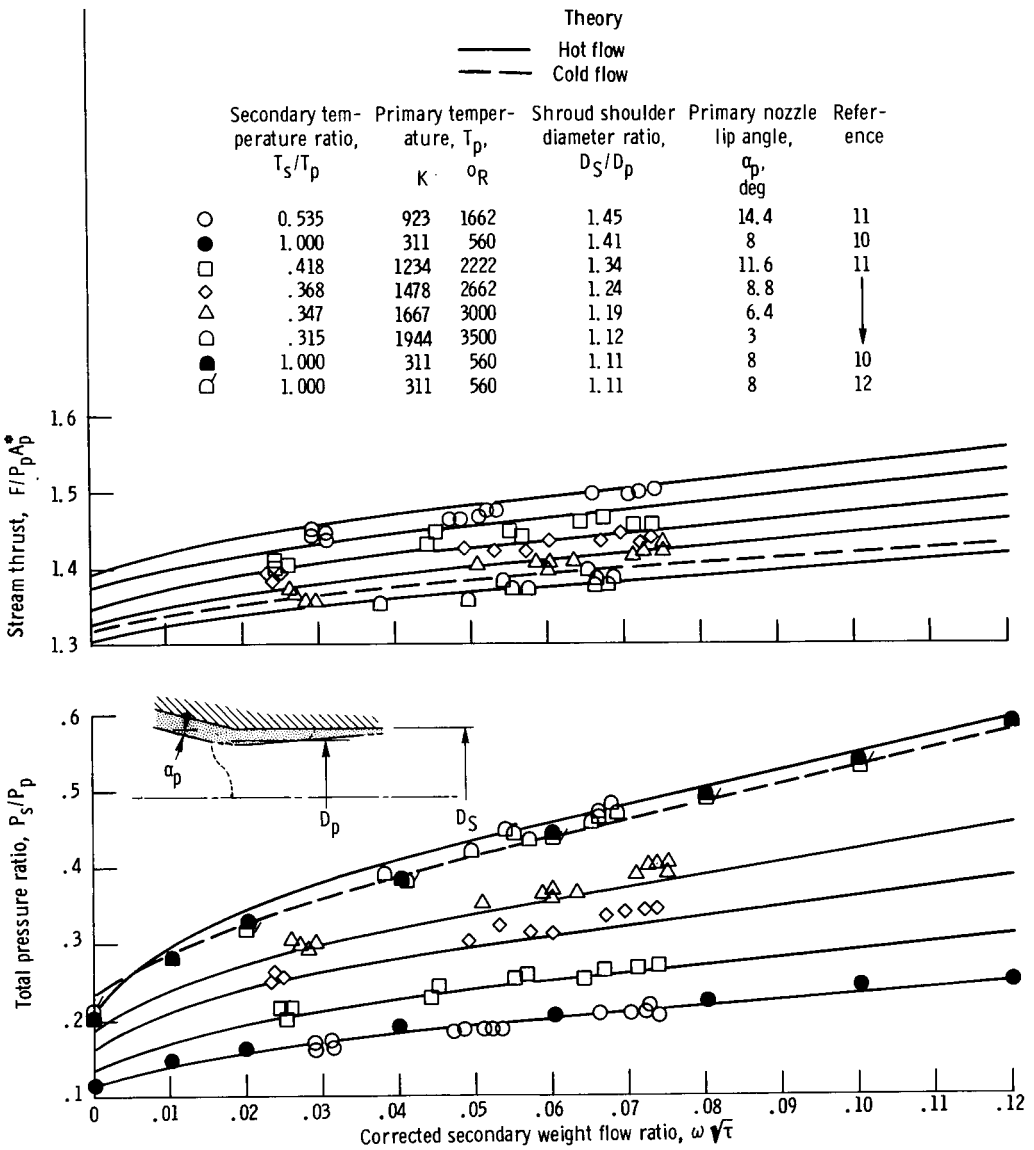

Figure 24. - Effect of primary temperature on performance of a cylindrical shroud ejector. Reynolds number, Re, 3.5x106.

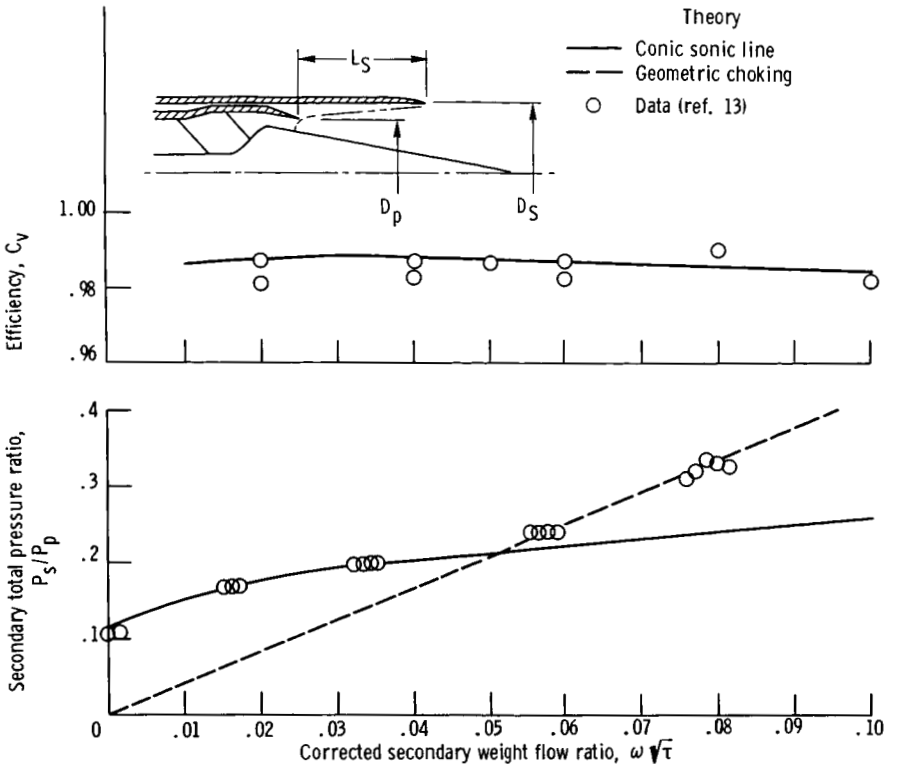

Figure 25. - Performance of a cylindrical shroud plug nozzle ejector - afterburning-on configuration. Shroud shoulder diameter ratio, D_S/D_p, 1.149; spacing ratio, L_S/D_p, 0.710; Reynolds number, Re, 3.5×10^6; ratio of primary total pressure to free-stream static pressure, P_p/p_0, 15.

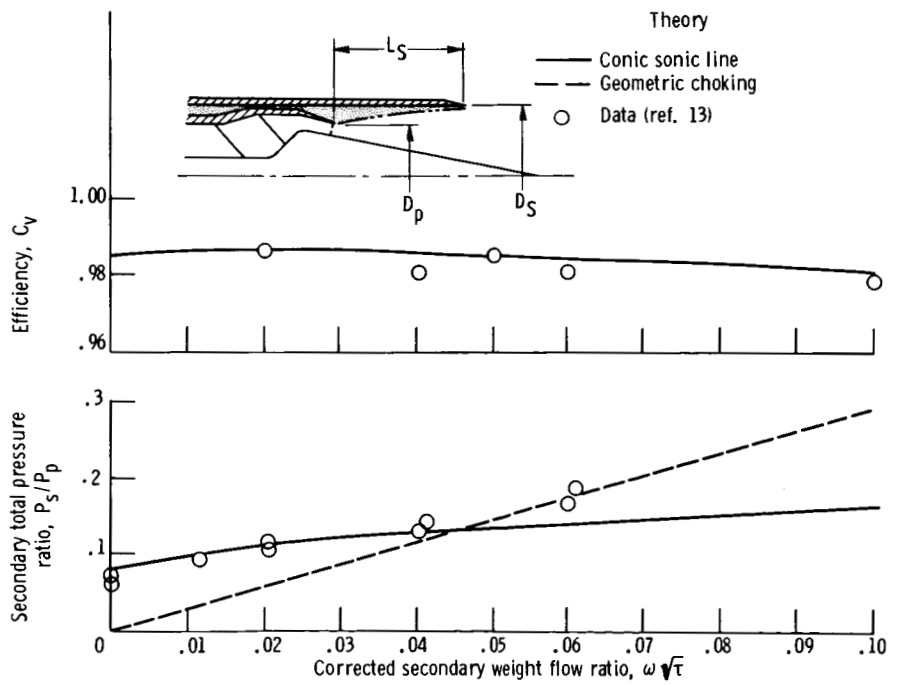

Figure 26. - Performance of a cylindrical shroud plug nozzle ejector - afterburning-on configuration. Shroud shoulder diameter ratio, D_S/D_p, 1.25; spacing ratio, L_S/D_p, 0.775; Reynolds number, Re, 3.5×10^6; ratio of primary total pressure to free-stream static pressure, P_p/p_0, 27.